ISLAMIC UNIVERSITY OF TECHNOLOGY

SPP PROPAGATION USING FDTD METHOD

by

Md. Azmot Ullah Khan
Md. Hosne Mobarok Shamim
Faisal Mahmud Fuad

A thesis submitted as a requirement for the degree of
Bachelor of Science in Electrical and Electronic Engineering

Supervised by
Md. Rakibul Hasan Sagor
Assistant Professor
Department of Electrical and Electronic Engineering
October 10, 2013

ISLAMIC UNIVERSITY OF TECHNOLOGY
Gazipur, Bangladesh

This thesis has been written by **Md. Azmot Ullah Khan**, **Md. Hosne Mobarok Shamim**, and **Faisal Mahmud Fuad** under the direction of **Md. Rakibul Hasan Sagor** as a requirement for the degree of **Bachelor of Science in Electrical and Electronic Engineering**.

_____

Prof. Dr. Md. Shahid Ullah
Head of the Department
Department of Electrical and
Electronic Engineering

_____

Md. Rakibul Hasan Sagor
Assistant Professor
(Thesis Supervisor)

_____

Md. Azmot Ullah Khan
(092425)

_____

Md. Hosne Mobarok Shamim
(092435)

_____

Faisal Mahmud Fuad (092431)

Dedicated to our respected Parents.

Acknowledgements

Abstract

SPP Propagation using FDTD Method
Electrical and Electronic Engineering
by
Md. Azmot Ullah Khan
Md. Hosne Mobarok Shamim
Faisal Mahmud Fuad

Now a days Surface Plasmon Polariton (SPP) has become a very attractive field of study for its extraordinary confinement of light at optical frequencies and its ability to overcome the diffraction limit. It is a very useful tool for the miniaturization of photonic devices. Keeping that in mind we have tried to discuss some of the basic ideas related to the SPP propagation. At first from various computational techniques FDTD has been taken for presenting the distribution of the electric and the magnetic field. With the help of FDTD 1-dimensional and 2-dimensinal simulations we get an idea how the signal behave within the dielectric at different frequencies. Next simulations related to SPP propagation are performed by forming the interface between metal and dielectric. Both the single and double interfaces are investigated with the help of Gaussian pulse signal. Lorentz model and Lorentz drude model are used for material modeling. Our aim was to enhance the power of the propagating signal. To do that grating has been considered. It is the periodic arrangement of different medium so that the propagating signal can be obstructed to couple with the main signal to enhance the power. We have tried to implement the grating structure with the help some numerical calculations taken from the published research papers. In our whole research work mainly two dielectrics (AlGaAs & GLS) have been used. For different metallic strip thickness transmission power has been shown. Lastly a comparison between the two dielectrics has been presented in terms of their transmission and loss properties.

Contents

List of Figures

List of Tables

Chapter 1

Introduction

Matter is a fundamental property of the material and light is a common source of energy. For thousands of years scientists are studying about these things to get something which is going to change the world. Einstein's photoelectric effect was a milestone in this regard. For thousands of years electron is ruling the world from the device point of view. Scientists are trying to create new dimensions using photons instead of electrons. It will miniaturize our devices as well as make it faster. They already have shown some of the results of their intellectual persuasion about Photonics. Still they are not satisfied. In the last decade the word SPP has evolved. It is a coupled state of electron and photon which has an extraordinary confinement of light. It is certainly better than photons but still have some challenging issues. The main problem is the distance of the power propagation and quick power dissipation. It has a huge prospect in communication, sensing and computing.

1.1 Literature Review

SPP requires some special computational technique for its efficient propagation. There are so many computational techniques through which electric and magnetic field can be designed within the material. The performance of a particular method depends on how accurately it can solve the differential equation. FDTD can be a good choice for its efficiency and cost effectiveness. Because of the ability to propagate in sub wavelength range SPP can be used extensively in nanoparticle propagation, nanowire propagation and Nano gap propagation. T. Onuki et al [23] investigated the propagation of SPP in Nanowires and Plasmon wave guides. For increasing the power the concept of coupling is very important. M. Hochberg et al [15] studied that light can be efficiently coupled between silicon wave guides and plasmonic waveguide with compact coupler. Bragg's grating plays a vital role in coupling the signals. Here in this thesis work Bragg's grating has been analyzed to enhance the power of the signal. The placement of grating should require a definite calculation to locate the fundamental local mode. In this research work a theoretical analysis of grating has been performed to calculate the grating length. The power transmission has also been analyzed for different metallic strip thicknesses and it is found maximum at $50nm$ strip length.

1.2 Computational Electromagnetic Technique

Electromagnetic analysis takes a lot of effort, money and time .Now a days simulation has become very popular because of the high costing on apparatus and other necessary staffs for the real time experiment. The simulations are almost accurate. Therefore the costing of the experiment can be reduced by reducing trial and error based experiment. Now we can do our experiment after being sure about the result.
There are two major computational techniques:

1. Analytical methods.

2. Numerical methods.

There are several analytical methods such as separation of variables, series expansion, con formal mapping, integration solution and perturbation. Numerical methods are consisting of some differential equation solver. We get approximate solution using this method.

1.2.1 Numerical Methods

From the ancient time people are using numerical analysis. Rhind Papyrus(1650 B.C) of ancient Egypt describes a root finding method for solving simple equation[6].Archimedes of Syearus(287-212 B.C) created much new mathematics, including the method of exhaustion for calculating lengths, areas and volumes of geometric figures[10].When used as a method to find approximate, it is in much the spirit of modern numerical integration and it was an important precursor to the development of the calculus by Isaac newton and Gott Fried Leibnitz.
In electromagnetic by numerical method we mean solving differential equation. There are a lot of efficient and cost effective ways of numerical techniques. The more accurate result gives a better performance. The performance of a method depends on it. There are several methods such as

1. Finite Difference Time Domain (FDTD)

2. Method of line (MOL)

3. The Beam Propagation Method (BPM)

4. Finite Element Method (FEM)

5. Transmission-Line-Matrix

6. Monte Carlo Method [20]

Method of line is a partial differential equation (PDE) solving technique [28],[12], and [27],.Here only one dimension is discretized. Scientist and Mathematician have worked hard to increase the accuracy and stability of this method.
Beam propagation method was introduced in the 1970's.It is a computational technique used in electromagnetic. It is used to solve Helmholtz equation under consideration of a time harmonic wave. It is an approximate technique. It simulates the propagation of light in a wave guide.
Finite element method is used to find the solution to the boundary value problem for differential

equations. The calculus of variations is used to minimize an error function and give a satisfactory solution. In this method the computational object is discretized into sub domain, named finite elements to approximate a more complex equation over a larger domain.

Transmission-line matrix (TLM) method is one of the most powerful time domain methods. It is based on the analogy between the electromagnetic field and a mesh of transmission lines. This method allows the 3-dimensional electromagnetic structures.

Finite Difference Time Domain Method was developed in 1966 by Kane Yee. His paper was published in IEEE transactions on Antennas and propagation. Now a days, this method is very much popular to compute electromagnetic equation. It is a time domain process. That is why it can compute a wide range of frequency. FDTD uses Maxwell's differential equation and implement it directly. For last two decade scientists and mathematicians are trying to improve the algorithm. With this method both linear and nonlinear material can be modeled. Different shapes of the materials can be modeled with this method. It is applicable in a wide range of spectrum (from microwave to visible light). We can model any problem related to radar signal technology, antennas, wireless communication devices, digital interconnects, Bio medical imaging or treatment, photonic crystals, nano Plasmonics etc. The results of the calculation done by this method are more accurate and robust. Now a days this method is a demanding computational electromagnetic technique.

1.3 Thesis Objective

Surface Plasmon Polariton has the extraordinary ability to confine light at optical frequencies [4],[7] , [11],[18], and [6] and its ability to overcome the diffraction limit [4],[7] , [11],[18], [19], and [10]. For SPP propagation a wave guide is required. Wave guide is created by forming the metal dielectric interface. Metal is very lossy in nature and for that reason the signal die out very quickly. Our objective is to increase the propagation distance of the signal by minimizing the loss when it propagates through the wave guide.

1.4 Thesis Organization

In Chapter 2 Theory of SPP propagation will be discussed. Basic Electromagnetic (EM) wave equation and its application in the single and double interface of metals and dielectrics will be elaborated as well. Chapter 3 deals with the different material modeling technique used to design the material. Here the modeling techniques will be explained mathematically. Among these techniques we used only Lorentz and Lorentz-Drude technique. In Chapter 4 FDTD method and its algorithm will be discussed. We will get to know the necessity of FDTD and its vast application in Electromagnetic modeling from the next chapter. FDTD method has been developed day by day. We will try to focus on the development of this method as well. We have used grating in some of the experiment we did so far. We will show the calculations related to it and its purpose in the material modeling in Chapter 5. We used different materials in our simulations. Finally we will compare those materials in different aspect of their properties in Chapter 6.

Chapter 2

SPP Propagation Theory

When light rays fall on any material then the electrons within the material excited. This excitation creates oscillation of electron within the metal. This collective oscillation is known as Plasmon and the coupled state between Plasmon and photon is known as Polariton. When Polariton travels through the interface between a conductor and a dielectric then the incident is called surface Plasmon Polariton. To visualize the propagation nature of SPP we have to get a clear understanding about the electromagnetic wave as SPP is considered as the electromagnetic excitation within the material. As the electromagnetic wave is characterized by the Maxwell's equation at the metal dielectric interface. The general form of Maxwell's equations are

$$\frac{\partial B}{\partial t} = -\nabla \times E \tag{2.1}$$

$$\frac{\partial D}{\partial t} = \nabla \times H \tag{2.2}$$

$$\nabla \cdot D = 0 \tag{2.3}$$

$$\nabla \cdot B = 0 \tag{2.4}$$

The electric and magnetic fields are related to the polarization (P) and magnetization (M) respectively. The relation between them are presented below

$$D = \varepsilon E \tag{2.5}$$

$$B = \mu H \tag{2.6}$$

For linear, isotropic and non-dispersive materials(materials having field independent, direction independent and frequency independent electric and magnetic properties) the relations between D to E and B to H can be simplified to

$$\frac{\partial H}{\partial t} = -\frac{1}{\mu} \nabla \times H \tag{2.7}$$

$$\frac{\partial E}{\partial t} = \frac{1}{\varepsilon} \nabla \times H \tag{2.8}$$

2.1 The EM wave propagation

Electromagnetic (EM) wave equation is mainly derived from the Maxwell's equation. Considering all the equations above let us take the curl operation for Faraday's law

$$\nabla \times (-\mu \frac{\partial H}{\partial t}) = \nabla \times \nabla \times E \tag{2.9}$$

Considering time derivative operation

$$-\mu \frac{\partial}{\partial t}(\nabla \times H) = \nabla \times \nabla \times E \tag{2.10}$$

Upon substitution of equation (2.8) in (2.10) we obtain

$$-\mu \frac{\partial}{\partial t}(\varepsilon \frac{\partial E}{\partial t}) = \nabla \times \nabla \times E \tag{2.11}$$

$$-\mu\varepsilon(\frac{\partial^2 E}{\partial t^2}) = \nabla \times \nabla \times E \tag{2.12}$$

By applying the rule we can simplify the right side of the above equation as

$$\nabla \times \nabla \times E = \nabla(\nabla \cdot E) - \nabla^2 E \tag{2.13}$$

By the Gauss's law it can be stated as the divergence of electric flux density for a charge free region is equal to zero.

$$\nabla \cdot D = \nabla \cdot \varepsilon E = \varepsilon(\nabla \cdot E) = 0 \Rightarrow \nabla \cdot E = 0 \tag{2.14}$$

Therefore,

$$\nabla \times \nabla \times E = 0 - \nabla^2 E \tag{2.15}$$

Substituting this in equation (2.12) gives

$$-\mu\varepsilon(\frac{\partial^2 E}{\partial t^2}) = -\nabla^2 E \tag{2.16}$$

The equation can be simplified to

$$\nabla^2 E - \mu\varepsilon(\frac{\partial^2 E}{\partial t^2}) = 0 \tag{2.17}$$

In case of magnetic field the equation can be written as

$$\nabla^2 H - \mu\varepsilon(\frac{\partial^2 H}{\partial t^2}) = 0 \tag{2.18}$$

For deriving the expression of electric field and magnetic field let us consider phase velocity which is defined as

$$\nu_p = \frac{\lambda}{T} \tag{2.19}$$

Phase velocity can be defined as the velocity at which wave propagates in space or simply the speed of the wave

$$\nu_p = \frac{1}{\sqrt{\mu\varepsilon}} \tag{2.20}$$

The general solution of EM wave that is harmonic in time and propagating in X direction is given in complex form

$$\psi(t, x) = Ae^{-j\omega t}e^{j\beta x} \tag{2.21}$$

Angular oscillation constant omega can be expressed as

$$\omega = \frac{2\pi}{T} \tag{2.22}$$

Angular phase constant beta can be expressed as

$$\beta = \frac{2\pi}{\lambda} \tag{2.23}$$

As the phase velocity Vp is related to both beta and omega.it can be written as

$$\nu_p = \frac{\lambda}{T} = \frac{\omega}{\beta} \tag{2.24}$$

Considering the Cartesian coordinate system electric and magnetic field can be expressed in three component i.e.

$$E = E_x.\overrightarrow{ax} + E_y.\overrightarrow{ay} + E_z.\overrightarrow{az} \tag{2.25}$$

$$H = H_x.\overrightarrow{ax} + H_y.\overrightarrow{ay} + H_z\overrightarrow{az} \tag{2.26}$$

If we calculate the partial derivative of the three components for the electric field and magnetic field then the components will be

$$\frac{\partial E_x}{\partial t} = \frac{1}{\varepsilon}\left(\frac{\partial H_z}{\partial y} - \frac{\partial H_y}{\partial z}\right) \tag{2.27}$$

$$\frac{\partial E_y}{\partial t} = \frac{1}{\varepsilon}\left(\frac{\partial H_x}{\partial z} - \frac{\partial H_z}{\partial x}\right) \tag{2.28}$$

$$\frac{\partial E_z}{\partial t} = \frac{1}{\varepsilon}\left(\frac{\partial H_y}{\partial x} - \frac{\partial H_x}{\partial y}\right) \tag{2.29}$$

$$\frac{\partial H_x}{\partial t} = \frac{1}{\mu}\left(\frac{\partial E_y}{\partial z} - \frac{\partial E_z}{\partial y}\right) \tag{2.30}$$

$$\frac{\partial H_y}{\partial t} = \frac{1}{\mu}\left(\frac{\partial E_z}{\partial x} - \frac{\partial E_x}{\partial z}\right) \tag{2.31}$$

$$\frac{\partial H_z}{\partial t} = \frac{1}{\mu}\left(\frac{\partial E_x}{\partial y} - \frac{\partial E_y}{\partial x}\right) \tag{2.32}$$

Figure 2.1: Fields Profile of SPPs at the Metal and Dielectric Interface.

2.2 Surface Plasmon Polariton

2.2.1 At Single Interface

The simplest geometry for SPP propagation can be presented by forming a single interface of a metal and a dielectric. The dielectric constant will have two parts: real part (signifying the propagation of the signal) and imaginary part (signifying loss of the signal).the generalized figure is shown by figure 2.1.

From faraday's law and Ampere's law we can get the two sets of equation for TE and TM wave. Those are:

1. For TE field equations are

$$\frac{\partial E_x}{\partial t} = \frac{1}{\varepsilon}\frac{\partial H_z}{\partial y} \tag{2.33}$$

$$\frac{\partial E_y}{\partial t} = -\frac{1}{\varepsilon}\frac{\partial H_z}{\partial x} \tag{2.34}$$

$$\frac{\partial H_z}{\partial t} = \frac{1}{\mu}\Big(\frac{\partial E_x}{\partial y} - \frac{\partial E_y}{\partial x}\Big) \tag{2.35}$$
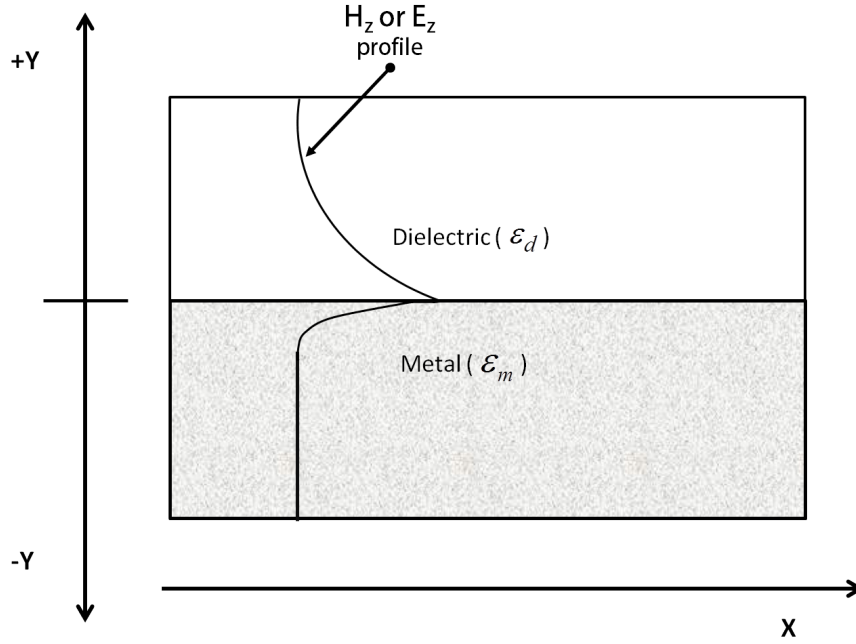
2. For TM field equations are

$$\frac{\partial H_x}{\partial t} = -\frac{1}{\mu}\frac{\partial E_z}{\partial y} \tag{2.36}$$

$$\frac{\partial H_y}{\partial t} = \frac{1}{\mu}\frac{\partial E_z}{\partial x} \tag{2.37}$$

$$\frac{\partial E_z}{\partial t} = \frac{1}{\varepsilon}\left(\frac{\partial H_y}{\partial x} - \frac{\partial H_x}{\partial y}\right) \tag{2.38}$$

In case of TE model let us assume Hz field propagating in x direction and decaying in y direction. The general solution for H_z will be

$$H_z = Ae^{-j\omega t}e^{j\beta x}e^{k|y|} \tag{2.39}$$

The relation between E_x and H_z can be stated as(2.32)

$$\frac{\partial E_x}{\partial t} = \frac{1}{\varepsilon}\frac{\partial H_z}{\partial y} \tag{2.40}$$

To solve the derivative we have to multiply $-j\omega$ to the time derivative and k with the derivative in y direction. The result is

$$-j\omega E_x = \frac{k}{\varepsilon}H_z \tag{2.41}$$

After rearranging the equation for E_x will be

$$E_x = \frac{Ak}{-j\omega\varepsilon}e^{-j\omega t}e^{j\beta x}e^{ky} \tag{2.42}$$

Similarly, E_y can be written as

$$E_y = \frac{A\beta}{-j\omega\varepsilon}e^{-j\omega t}e^{j\beta x}e^{ky} \tag{2.43}$$

The tangential field of the dielectric will be

$$E_x = \frac{A_d k_d}{-j\omega\varepsilon_d}e^{-j\omega t}e^{j\beta x}e^{k_d y} \tag{2.44}$$

$$H_z = A_d e^{-j\omega t}e^{j\beta x}e^{k_d y} \tag{2.45}$$

Similarly, the tangential field of the metal will be

$$E_x = \frac{A_m k_m}{-j\omega\varepsilon_m}e^{-j\omega t}e^{j\beta x}e^{k_m y} \tag{2.46}$$

$$H_z = A_m e^{-j\omega t}e^{j\beta x}e^{k_m y} \tag{2.47}$$

Considering $A_d = A_m$
At the interface $E_x$will be equal to

$$\frac{k_d}{k_m} = -\frac{\varepsilon_d}{\varepsilon_m} \tag{2.48}$$

It is clear from the above discussion that the permittivity will have different sign to propagate and the wave equation should satisfy in both the media. Substituting the value of H_z in (2.18) for dielectric gives

$$-\beta^2 H_z + k_d^2 H_z + \mu\varepsilon_d\omega^2 H_z = 0 \tag{2.49}$$

$$\beta^2 = k_d^2 + \mu\varepsilon_d\omega^2 \tag{2.50}$$

For the metal result will be

$$\beta^2 = k_m^2 + \mu\varepsilon_m\omega^2 \tag{2.51}$$

Substituting (2.48) in (2.50) gives

$$\beta^2 = (\frac{\varepsilon_d}{\varepsilon_m})^2 k_m^2 + \mu\varepsilon_d\omega^2 \tag{2.52}$$

Multiplying equation (2.52) by the constant $\frac{\varepsilon_d}{\varepsilon_m}$ gives

$$-(\frac{\varepsilon_d}{\varepsilon_m})^2\beta^2 = -(\frac{\varepsilon_d}{\varepsilon_m})^2 k_m^2 - (\frac{\varepsilon_d}{\varepsilon_m})^2\mu\varepsilon_m\omega^2 \tag{2.53}$$

Combining (2.52) and (2.53) together gives

$$\beta^2(1 - (\frac{\varepsilon_d}{\varepsilon_m})^2) = (\varepsilon_d - (\frac{\varepsilon_d}{\varepsilon_m})^2\varepsilon_m)\mu\omega^2 \tag{2.54}$$

This equation can be reduced to

$$\beta^2(1 - \frac{\varepsilon_d}{\varepsilon_m})(1 + \frac{\varepsilon_d}{\varepsilon_m}) = (1 - \frac{\varepsilon_d}{\varepsilon_m})\mu\varepsilon_d\omega^2 \tag{2.55}$$

Rearranging the equation gives

$$\beta^2 = \frac{\mu\varepsilon_d\omega^2}{1 + \frac{\varepsilon_d}{\varepsilon_m}} \tag{2.56}$$

$$\beta^2 = \omega^2\mu\frac{\varepsilon_d\varepsilon_m}{\varepsilon_d + \varepsilon_m} \tag{2.57}$$

Taking the square root gives the following

$$\beta = \omega\sqrt{\mu\frac{\varepsilon_d\varepsilon_m}{\varepsilon_d + \varepsilon_m}} \tag{2.58}$$

For the TM case, where we have the fields E_z, H_x and H_y, we start with E_z going by

$$E_z = Ae^{-j\omega t}e^{j\beta x}e^{k|y|} \tag{2.59}$$

Magnetic component can be stated as

$$H_x = \frac{k}{j\omega\mu}E_z \tag{2.60}$$

$$H_y = \frac{\beta}{\omega\mu}E_z \tag{2.61}$$

Hx and Ez are tangential to the interface and in the dielectric side they are equal to

$$H_x = \frac{A_dk_d}{j\omega\mu}e^{-j\omega t}e^{j\beta x}e^{k_dy} \tag{2.62}$$

$$E_z = Ae^{-j\omega t}e^{j\beta x}e^{k_dy} \tag{2.63}$$
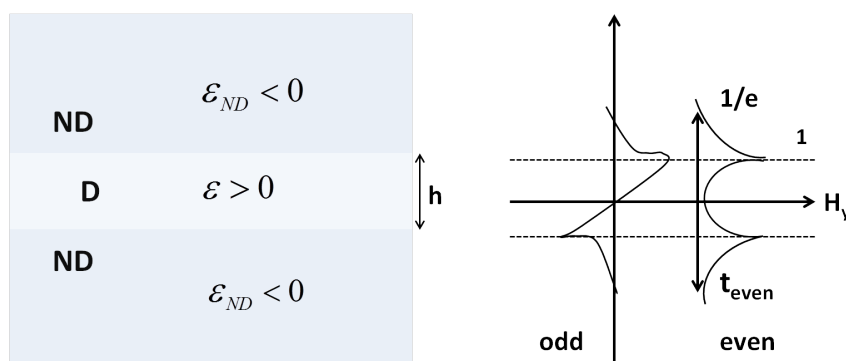
Figure 2.2: Field Profile in a Double Interface Metal-Dielectric-Metal.

In the metal side, they are

$$H_x = -\frac{A_m k_m}{j\omega\mu} e^{-j\omega t} e^{j\beta x} e^{k_m y} \tag{2.64}$$

$$E_z = A_m e^{-j\omega t} e^{j\beta x} e^{k_m y} \tag{2.65}$$

Considering $A_d = A_m$

$$Ak_d = -Ak_m \tag{2.66}$$

$$A(k_d + k_m) = 0 \tag{2.67}$$

Value of k has to be greater than zero to have a decaying field at the interface and the amplitude of the field is equal to zero. Therefore no SPP is there for TM mode.

2.3   Double Interface

For efficient transmission to overcome the decay of the signal more than one interface can be formed. Two types of structures can be formed such as MDM and DMD. Here fields from both sides interact to form the coupled mode. The structure for double interface is presented by figure 2.2.

Chapter 3

Material Modeling

Metals are good conductors at low frequency. At high frequency they exhibit some dispersion property. With the increase of the frequency the metal turns into a dielectric. SPP is produced at the interface of the metal and dielectric. Therefore it is vital that we study the material. The material can be modeled using different modeling techniques.

Inside any material, the relationship between the three vectors D (electrical flux density), E (electric field intensity) and P (polarization density) can determine its behavior in the presence of an oscillating external electromagnetic field. For any material, the following equations apply [3].

$$D = \epsilon E \tag{3.1}$$

$$P = \varepsilon_0 \chi E \tag{3.2}$$

$$D = \varepsilon_0 E + P \tag{3.3}$$

where, ϵ is the permittivity, which is a physical quantity that describes the material's ability to transmit an electric field. In SI units, the permittivity is measured in Farads per meter (F/m).

χ is the susceptibility, which is a physical quantity of a dielectric material that measures how easily it is polarized in response to an applied electric field, and it is a dimensionless quantity.

The relationship between permittivity and susceptibility can be found by substituting P in equations (3.2) and (3.3).

$$D = \varepsilon_0 E + \varepsilon_0 \chi E \tag{3.4}$$

Taking E as a common factor

$$D = \varepsilon_0 (1 + \chi) E \tag{3.5}$$

and combining (3.5) and (3.1) yields

$$\varepsilon = \varepsilon_0 (1 + \chi) \tag{3.6}$$

The final relation between ϵ and χ is also valid in the frequency domain

$$\varepsilon(\omega) = \varepsilon_0 (1 + \chi(\omega)) \tag{3.7}$$

The relative permittivity is given as

$$\varepsilon_r(\omega) = 1 + \chi(\omega) \tag{3.8}$$

For a dispersive material, the frequency dependent permittivity and susceptibility are to be modeled perfectly in order to get the perfect response of the material for certain electromagnetic excitation. To model a dispersive material, different models such as the Drude model, Lorentz model, Debye model and Lorentz-Drude model are widely used. In the following subsections these models are briefly described.

3.1 The Drude Model

The Drude model was given by Paul Drude in 1900 [8] [9]. In Drude's model the metal is described as a volume filled with stationary positive ions immersed in a gas of electrons following the kinetic theory of gases. These electrons can travel inside metal freely without any interaction with each other. It happens due to the charge shielding effect. There are two forces acting on the metals;

1. Driving force F_d,

2. Damping force F_g.

The driving force and the damping force can be expressed as

$$F_d = qE = -eE \tag{3.9}$$

$$F_g = \Gamma v \tag{3.10}$$

Their direction of action is opposite to each other. Therefore the resultant force becomes,

$$F = F_d - F_g \tag{3.11}$$

Using Newton's first law of motion,

$$mr'' = -eE + \Gamma r' \tag{3.12}$$

where,

m: mass of an electron.
Γ: damping constant in Newton second per meter.
r: displacement in meter.
v: velocity of the electron.
q: electron's charge.
The time harmonic electric field and displacement can be expressed as

$$E(t) = E_0 e^{-j\omega t} \Leftrightarrow E(\omega) \tag{3.13}$$

$$r(t) = R_0 e^{-j\omega t} \Leftrightarrow R(\omega) \tag{3.14}$$

The Fourier transform of (3.12)is

$$mR''(\omega) - \Gamma mR'(\omega) + eE = 0 \tag{3.15}$$

Writing the derivatives of the above equation in the frequency domain

$$-mR''(\omega) + jm\Gamma R(\omega) + eE = 0 \tag{3.16}$$

Simplifying the above equation and solving for R gives

$$R(\omega) = \frac{-e}{m(j\Gamma\omega - \omega^2)} E(\omega) \tag{3.17}$$

The polarization for n electrons can be expressed as

$$P(\omega) = -neR(\omega) \tag{3.18}$$

So from (3.17) and (3.18) we can write

$$P(\omega) = \frac{ne^2}{m(j\Gamma\omega - \omega^2)} E(\omega) \tag{3.19}$$

From the above equation an expression for the susceptibility can be obtained as

$$\frac{P(\omega)}{\varepsilon_0 E(\omega)} = \frac{ne^2}{\varepsilon_0 m(j\Gamma\omega - \omega^2)} = \chi(\omega) \tag{3.20}$$

Substituting equation (3.20) in equation (3.8) yields

$$\varepsilon_r = 1 + \frac{ne^2}{\varepsilon_0 m(j\Gamma\omega - \omega^2)} \tag{3.21}$$

As the plasma frequency ω_p is given by $\omega_p^2 = \frac{ne^2}{\epsilon_0 m}$ the above equation can be written as

$$\varepsilon_r(\omega) = 1 + \frac{\omega_p^2}{j\Gamma\omega - \omega^2} E(\omega) \tag{3.22}$$

So from equation (3.1) the frequency dependent electric flux density becomes

$$D(\omega) = \varepsilon_0 (1 + \frac{\omega_p^2}{j\Gamma\omega - \omega^2}) E(\omega) \tag{3.23}$$

For low frequencies $\Gamma\omega << 1$. So equation (3.23) is reduced to

$$D(\omega) = \varepsilon_0 (1 - \frac{\omega_p^2}{\omega^2}) E(\omega) \tag{3.24}$$

The above relationship is known as the Drude Model.

3.2 The Lorentz Model

The Lorentz model is a simpler representation of atom. Using this model we can visualize the interaction between atom and field. Lorentz showed here a connection between the nucleus and electron. Here both of them are masses. Therefore there is a force acting between them. This force is denoted by F_r.

$$F_r = -kr \tag{3.25}$$

where, k is the spring constant (N/m).
So (3.15) can be written as

$$mr'' + \Gamma mr' + mkr + eE = 0 \tag{3.26}$$

By doing Fourier analysis we get,

$$R(\omega)(m\omega_0^2 + j\omega m\Gamma - m\omega^2) = eE(\omega) \tag{3.27}$$

where, $\omega_0 = \sqrt{\frac{k}{m}}$
(3.27) can be used to find $R(\omega)$ in terms of $E(\omega)$

$$R(\omega) = \frac{-e}{m(\omega_0^2 + j\omega\Gamma - \omega^2)} E(\omega) \tag{3.28}$$

Using equation (3.18) and equation (3.28) the susceptibility is found to be

$$\frac{P(\omega)}{\varepsilon_0 E(\omega)} = \frac{ne^2}{\varepsilon_0 m(\omega_0^2 + j\omega\Gamma - \omega^2)} = \chi(\omega) \tag{3.29}$$

Combining equation (3.1) and equation (3.8), the expression for D in the frequency domain becomes

$$D(\omega) = \varepsilon_0(1 + \frac{\omega_p^2}{\omega_0^2 + j\omega\Gamma - \omega^2})E(\omega) \tag{3.30}$$

The above relationship is known as the Lorentz model.

3.3 The Lorentz-Drude Model

When an EM field is applied to a metal, the electrons oscillate inside the metal. There are two electrons here. One is the free electron and other one is the bound electron. Free electrons cause the permittivity in the Drude model and the bound electrons causes the permittivity in the Lorentz model. The permittivity in the LD model is given by

$$\varepsilon = \varepsilon_{free} + \varepsilon_{bound} \tag{3.31}$$

For the free electrons, permittivity is

$$\varepsilon_{free} = 1 + \frac{\omega_p}{j\omega\Gamma + \omega^2} \tag{3.32}$$

and for bound electrons, permittivity is

$$\varepsilon_{bound} = \frac{\omega_p}{\omega_0 + j\omega\Gamma + \omega^2} \tag{3.33}$$

Combining both models together yields

$$D(\omega) = \varepsilon_0(1 + \frac{\omega_p}{j\omega\Gamma - \omega^2} + \frac{\omega_p}{\omega_0 + j\omega\Gamma - \omega^2}) \tag{3.34}$$

3.4 The Debye Model

The Debye model was first developed by Peter Debye in the year 1912. According to the Debye model, materials are assumed to have electric dipoles and when the electric field is applied, these dipoles follow the behavior of the field having some relaxation time. The polarization will have greater strength if the electric field oscillates at a slow frequency, whereas a fast oscillating field causes low polarization. Since metals have very short relaxation times, the polarization in metals is strong.
If a DC electric field is applied to a dielectric, the polarization takes some time to follow the electric field. The instantaneous polarization $P(t)$is given by

$$P(t) = P_\infty(1 - e^{-t/\tau}) \tag{3.35}$$

where, P_∞ is the polarization in DC steady state and τ is the time constant.
The derivative of equation (3.35) is

$$\frac{dP(t)}{dt} = \frac{1}{\tau}P_\infty e^{-t/\tau} \tag{3.36}$$

Combining equation (3.35) and equation (3.36) yields

$$P(t) = P_\infty - \frac{dP(t)}{dt} \tag{3.37}$$

Since $P_\infty = \epsilon_0(\epsilon - 1)E(t)$, equation (3.37) reduced to

$$P(t) = \varepsilon_0(\varepsilon - 1)E(t) - \tau\frac{dP(t)}{dt} \tag{3.38}$$

The Fourier analysis of equation (3.38) is

$$\varepsilon_0(\varepsilon - 1)E(\omega) = P(\omega) + j\omega\tau P(\omega) \tag{3.39}$$

The linear susceptibility is expressed as

$$\frac{(\varepsilon - 1)}{1 + j\omega\tau} = \frac{P(\omega)}{\varepsilon_0 E(\omega)} = \chi(\omega) \tag{3.40}$$

From equation (3.8) the permittivity becomes

$$\varepsilon_r(\omega) = \chi(\omega) + 1 = \frac{(\varepsilon - 1)}{1 + j\omega\tau} + 1 \tag{3.41}$$

$$\varepsilon_r(\omega) = \varepsilon_\infty + \frac{\varepsilon_s - \varepsilon_\infty}{1 + j\omega\tau} \tag{3.42}$$

Another term related to the conductivity of metal is added to the above equation. Equation (3.42) can be expanded as

$$\varepsilon_r(\omega) = \varepsilon_\infty + \frac{\varepsilon_s - \varepsilon_\infty}{1 + j\omega\tau} - j\frac{\sigma}{\omega\varepsilon_0} \tag{3.43}$$

If the model is represented in terms of its real and imaginary parts, then,

$$\varepsilon_r(\omega) = \varepsilon'(\omega) - j\varepsilon''(\omega) \tag{3.44}$$

Chapter 4

Material modeling using FDTD method

4.1 Introduction to FDTD

FDTD stands for Finite Difference Time Domain method. It is a widely used and most popular electromagnetic equation solution technique. In this method the object is splitted into numerous parts and then integrated together. It is a time domain method. That is why it can work with a wide range of frequency. In our case we are dealing with high frequency propagation which becomes very much easy in FDTD method. It does not require a lot of memory to store the data. It has a recursive algorithm which makes it possible to store the whole data in a small memory. FDTD follows the Yee's mesh. This method was first established by Kane Yee in 1966.

FDTD method is formulated from the Maxwell's equation. For a non-dispersive and linear isotropic material the Maxwell's equation can be showed as follows,

$$\frac{\partial H}{\partial t} = -\frac{1}{\mu} \nabla \times E \tag{4.1}$$

$$\frac{\partial E}{\partial t} = \frac{1}{\varepsilon} \nabla \times H \tag{4.2}$$

From (4.1) and (4.2) we get

$$\frac{\partial E_z}{\partial y} - \frac{\partial E_y}{\partial z} = j\omega\mu_0 H_x \tag{4.3}$$

$$\frac{\partial E_x}{\partial z} - \frac{\partial E_z}{\partial x} = j\omega\mu_0 H_y \tag{4.4}$$

$$\frac{\partial E_y}{\partial x} - \frac{\partial E_x}{\partial y} = j\omega\mu_0 H_z \tag{4.5}$$

$$\frac{\partial H_z}{\partial y} - \frac{\partial H_y}{\partial z} = -j\omega\varepsilon_r E_x \tag{4.6}$$

$$\frac{\partial H_x}{\partial z} - \frac{\partial H_z}{\partial x} = -j\omega\varepsilon_r E_y \tag{4.7}$$
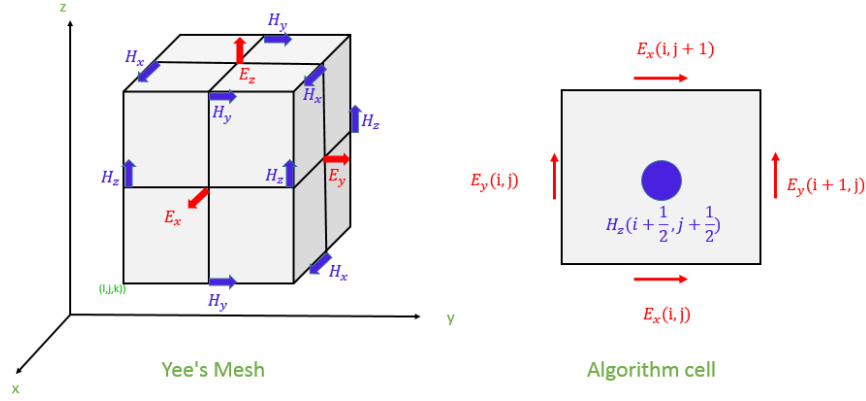
Figure 4.1: Yee's Spatial Grid.

$$\frac{\partial H_y}{\partial x} - \frac{\partial H_x}{\partial y} = -j\omega\varepsilon_r E_z \tag{4.8}$$

FDTD method is based on these six equations (4.3) to (4.8).

This method calculates the electric field and magnetic fields in both time and space, rather than by solving the wave equation for either the electric field or the magnetic field alone.

Yee's FDTD scheme splits Maxwell's curl equations. It approximates the time and Space first order partial derivatives with central differences, and then solves the resulting Equations by using a leapfrog scheme [13].

4.2 Yee's mesh

From 4.1 we can understand that there are both Ampere's law and Faraday's law contour are present. E and H components are positioned at the centers of the grid lines and surfaces such that each component is surrounded by four components. This gives a simple picture of three dimensional space being filled by interlinked arrays of Faraday's law and Ampere's law contours. Thus, it is possible to identify the E components related with the displacement of the current flux linking with the H loops and, correspondingly, the H components related with the magnetic flux are linked with the E loops, as shown by 4.2.

Assuming only two dimensional space there is no component in z direction. Therefore we have,

$$\frac{\partial H_y}{\partial z} = 0, \frac{\partial H_x}{\partial z} = 0, \frac{\partial E_x}{\partial z} = 0, \frac{\partial E_y}{\partial z} = 0 \tag{4.9}$$

From equation (4.3) to (4.8), we can write two independent sets of coupled equations.

For TM polarized field,

$$\frac{\partial E_x}{\partial t} = \frac{1}{\varepsilon}\frac{\partial H_z}{\partial y} \tag{4.10}$$

$$\frac{\partial E_y}{\partial t} = -\frac{1}{\varepsilon}\frac{\partial H_z}{\partial x} \tag{4.11}$$

$$\frac{\partial H_z}{\partial t} = \frac{1}{\mu}\left(\frac{\partial E_x}{\partial y} - \frac{\partial E_y}{\partial x}\right) \tag{4.12}$$
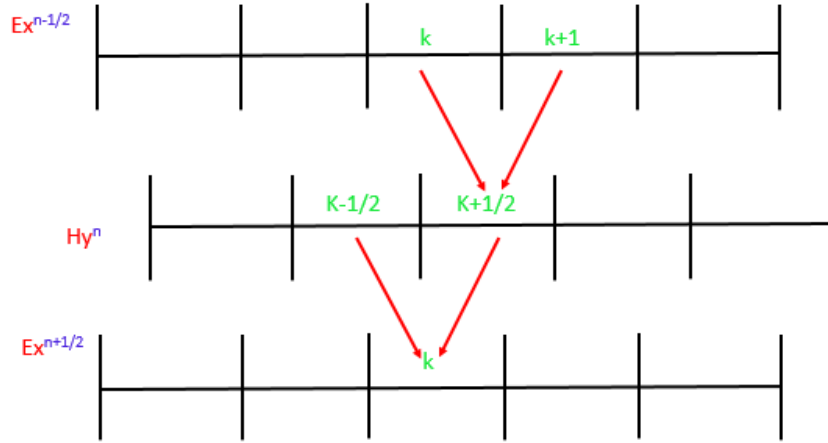
Figure 4.2: Leapfrog scheme: the temporal scheme of the FDTD method.

For TE polarized field,

$$\frac{\partial H_x}{\partial t} = -\frac{1}{\mu}\frac{\partial E_z}{\partial y} \tag{4.13}$$

$$\frac{\partial H_y}{\partial t} = -\frac{1}{\mu}\frac{\partial E_z}{\partial x} \tag{4.14}$$

$$\frac{\partial E_z}{\partial t} = \frac{1}{\varepsilon}\left(\frac{\partial H_y}{\partial x} - \frac{\partial H_x}{\partial y}\right) \tag{4.15}$$

Utilizing Yee's spatial grid scheme, the partial spatial derivatives in (4.10) and (4.12) can be approximated by a central difference approximation in space. For example, equations (4.10) and (4.12) respectively become

$$\frac{\partial E_x}{\partial t} = \frac{1}{\varepsilon}\frac{H_z(i,j) - H_z(i,j-1)}{\Delta y} \tag{4.16}$$

$$\frac{\partial E_y}{\partial t} = -\frac{1}{\varepsilon}\frac{H_z(i,j) - H_z(i-1,j)}{\Delta x} \tag{4.17}$$

$$\frac{\partial H_z}{\partial t} = \frac{1}{\mu}\left(\frac{E_x(i,j+1) - E_x(i,j)}{\Delta y} - \frac{E_y(i+1,j) - E_y(i,j)}{\Delta x}\right) \tag{4.18}$$

Yee's algorithm also utilizes central difference in time for the E and H components. The E and H components are solved by using a leapfrog algorithm as shown in 4.2. All of the E components in the modeled space are computed and stored in memory by using the previously computed values of E and the newly computed H field data. At the next step, H is recomputed based on the previously obtained H and the newly updated E. This process continues until the time-stepping is terminated.

Applying central difference approximation equation (4.16) and (4.18) respectively, become

$$\frac{E_x^{n+1}(i+\frac{1}{2},j) - E_x^n(i+\frac{1}{2},j)}{\Delta t} = \frac{1}{\varepsilon}\frac{H_z^{n+\frac{1}{2}}(i+\frac{1}{2},j+\frac{1}{2}) - H_z^{n+\frac{1}{2}}(i+\frac{1}{2},j-\frac{1}{2})}{\Delta y} \tag{4.19}$$

19

$$\frac{E_y^{n+1}(i,j+\frac{1}{2}) - E_y^n(i,j+\frac{1}{2})}{\Delta t} = \frac{1}{\varepsilon}\frac{H_z^{n+\frac{1}{2}}(i+\frac{1}{2},j+\frac{1}{2}) - H_z^{n+\frac{1}{2}}(i-\frac{1}{2},j+\frac{1}{2})}{\Delta y} \quad (4.20)$$

$$\frac{H_z^{n+\frac{1}{2}}(i+\frac{1}{2},j+\frac{1}{2}) - H_z^{n-\frac{1}{2}}(i+\frac{1}{2},j+\frac{1}{2})}{\Delta t} = \frac{1}{\mu}\frac{E_x^n(i+\frac{1}{2},j+1) - E_x^n(i+\frac{1}{2},j)}{\Delta y} - \frac{E_y^n(i+1,j+\frac{1}{2}) - E_y^n(i,j+\frac{1}{2})}{\Delta x}$$
$$(4.21)$$

In three dimensions Courant Friedrich Levy (CFL) stability condition is

$$\Delta t \leq t_{\max} = \frac{1}{c\sqrt{\frac{1}{\Delta x^2} + \frac{1}{\Delta y^2} + \frac{1}{\Delta z^2}}} \quad (4.22)$$

4.3   Dispersion of the Material in FDTD

The FDTD method, which is a robust numerical modeling technique, has been commonly used for modeling electromagnetic wave interaction with complex materials. One of the most major developments in the FDTD method is its ability to model dispersive materials. As most of the dielectrics and metals are dispersive, modeling materials in FDTD requires the knowledge of modeling dispersive materials, which were discussed in chapter 3. There are three main methods to model dispersive materials in the FDTD:

1. The recursive convolution (RC) method.

2. The auxiliary differential equation (ADE) method.

3. The Z-transform method.

In this chapter, the ADE dispersive FDTD method will be discussed in detail and applied to model metals and dielectric materials.

4.3.1   Auxiliary differential method

The auxiliary differential method was first introduced by Allen Taflove [26]. The idea was to convert the frequency domain relationship into time domain relationship. This method is very popular because of its high flexibility to fit the permittivity function. To get the time domain representation between D and E we can start with the frequency domain relationship

$$D(\omega) = \varepsilon_0 \frac{\sigma}{j\omega} E(\omega) \quad (4.23)$$

Which can be simplified to

$$j\omega D(\omega) = \varepsilon_0 \sigma E(\omega) \quad (4.24)$$

With the application of inverse Fourier transform the above equation becomes

$$\frac{dD(t)}{dt} = \varepsilon_0 \sigma E(t) \quad (4.25)$$

Discretizing the above relation using forward difference scheme

$$\frac{D^{n+1} - D^n}{\Delta t} = \varepsilon_0 \sigma E^{n+1} \tag{4.26}$$

The updated equation of E will be

$$E^{n+1} = \frac{D^{n+1} - D^n}{\varepsilon_0 \sigma \Delta t} \tag{4.27}$$

4.3.2 The General Algorithm

There are different algorithms to design different materials. Deriving of FDTD equation for one term and one pole dispersion is easy. For multi pole dispersion relation such as LD 6 pole it is very difficult to derive FDTD equation because of its long derivation and larger memory requirement. Allen Taflove proposed matrix inversion technique to solve the multiple poles. This technique is also impractical. When there are two or more different materials with different dispersion relation present within the space then separate algorithm is required to describe each dispersion relation [29]. For this reason a separate algorithm has been presented by Dr. Mohammad A. Al-Sunaidi and Ahmad Ali Al Jabr [2] based on the ADE method. The dispersion relation takes the general form as

$$D(\omega) = \varepsilon(\omega)E(\omega) \tag{4.28}$$

Which can also be expressed as

$$D(\omega) = \varepsilon_0 \varepsilon_\infty E(\omega) + \sum_i^N P_i(\omega) \tag{4.29}$$

The equation is in frequency domain. Upon application of Fourier transform we get

$$D^n = \varepsilon_0 \varepsilon_\infty E^n + \sum_i^N P_i^n \tag{4.30}$$

Solving for electric field (E)
In case of Lorentz pole the dispersion relation can be stated as

$$P(\omega) = \frac{a}{b + jc\omega - d\omega^2} E(\omega) \tag{4.31}$$

Multiplying by denominator, the equation becomes

$$.(b + jc\omega - d\omega^2)P(\omega) = aE(\omega) \tag{4.32}$$

Converting in time domain from frequency domain we get

$$.bP(t) + cP'(t) + dP''(t) = aE(t) \tag{4.33}$$

Considering time derivative of equation (4.28) at any time instant n, the updated equation of polarization can be obtained. The resulting discretized equation will be

$$bP^n + c\frac{P^{n+1} - P^{n-1}}{2\Delta t} + d\frac{P^{n+1} - 2P^n + P^{n-1}}{\Delta t^2} = aE^n \tag{4.34}$$

21

Table 4.1: General Algorithm Constants Using ADE

Dispersion term in frequency domain	C_1	C_2	C_3
Lorentz Pole $P = \frac{a}{b+jc\omega-d\omega^2}E$	$\frac{4d-2b\Delta t^2}{2d+c\Delta t}$	$\frac{-2d+c\Delta t}{2d+c\Delta t}$	$\frac{2a\Delta t^2}{2d+c\Delta t}$
Drude Pole $P = \frac{a}{jc\omega-d\omega^2}E$	$\frac{4d}{2d+c\Delta t}$	$\frac{-2d+c\Delta t}{2d+c\Delta t}$	$\frac{2a\Delta t^2}{2d+c\Delta t}$
Plasma Frequency $P = \frac{a}{\omega^2}E$	2	-1	$2a\Delta t^2$
Debye term $P = \frac{a}{b+jc\omega}E$	$-\frac{2b\Delta t}{c}$	1	$\frac{2a\Delta t}{c}$
Conductivity term $P = \frac{a}{jc\omega}E$	0	1	$\frac{2a\Delta t}{c}$

The above equation can be solved for P^{n+1} in terms of P^n, P^{n+1}, E^n

$$P^{n+1} = \frac{4d-2b\Delta t^2}{2d+c\Delta t}P^n + \frac{-2d+c\Delta t}{2d+c\Delta t}P^{n-1} + \frac{2a\Delta t^2}{2d+c\Delta t}E^n \qquad (4.35)$$

Which can be represented in simpler form as

$$P^{n+1} = C_1 P^n + C_2 P^{n-1} + C_3 E^n \qquad (4.36)$$

Where,

$$C_1 = \frac{4d-2b\Delta t^2}{2d+c\Delta t}, C_2 = \frac{-2d+c\Delta t}{2d+c\Delta t}, C_3 = \frac{2a\Delta t^2}{2d+c\Delta t} \qquad (4.37)$$

These C_1, C_2 and C_3 values will differ from material to material. The values of these constants for different models are presented in table 4.1.

4.3.3 Absorbing Boundary Conditions

When the simulation is performed then the computational domain needs to be terminated otherwise it is not possible to simulate the propagation to infinity. Terminating the propagation means that the electric field will be zero. So there should be some arrangement so that the electric field can be forced to stop propagating at certain distance.

For this purpose Berenger [5] proposed a model which is known as perfectly matched layer (PML). With the help of this layer electric field can be attenuated very rapidly until it becomes zero. Two quantities have been introduced which are $sigma$ and $sigma*$ to describe the equations inside the PML. The equations are

$$\varepsilon_0 \frac{\partial E_x}{\partial t} + \sigma E_x = \frac{\partial H_z}{\partial y} \qquad (4.38)$$

$$\varepsilon_0 \frac{\partial E_y}{\partial t} + \sigma E_y = -\frac{\partial H_z}{\partial x} \qquad (4.39)$$

$$\mu_0 \frac{\partial H_z}{\partial t} + \sigma^* H_z = \left(\frac{\partial E_x}{\partial y} - \frac{\partial E_y}{\partial x}\right) \qquad (4.40)$$
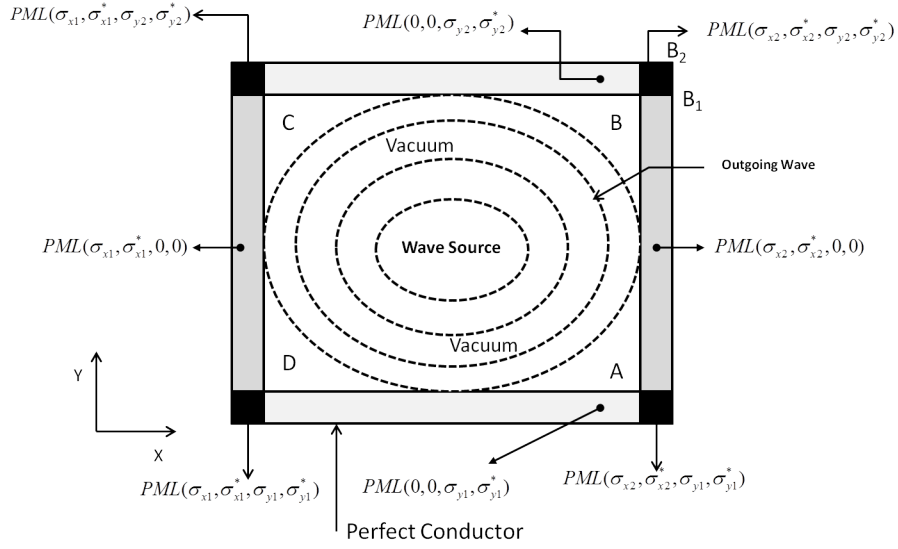
Figure 4.3: PML Setup

When the wave travels from one medium to another medium, no reflection will occur if the impedance of the two mediums are equal. This is known as the impedance matching. Following equation can be obtained from this condition

$$\frac{\sigma}{\varepsilon_0} = \frac{\sigma^*}{\mu_0} \tag{4.41}$$

However the problem is concerning only with the normal incidence but we have to consider all forms of incidence. So the H_z field is distributed into two components H_{zx} and H_{zy} where one is normal and another one is tangential to the PML. If we apply this to FDTD, it means to split $sigma^*$ into $sigma_x^*$ and $sigma_y^*$ where the first deal with H_{zy} and H_{zx}. If we split equation (4.40) three components of the equation wiil be evolved

$$\mu_0 \frac{\partial H_{zx}}{\partial t} + \sigma_x^* H_{zx} = -\frac{\partial E_y}{\partial x} \tag{4.42}$$

$$\mu_0 \frac{\partial H_{zy}}{\partial t} + \sigma_y^* H_{zy} = -\frac{\partial E_x}{\partial y} \tag{4.43}$$

$$H_z = H_{zx} + H_{zy} \tag{4.44}$$

In the computational domain $sigma_x^*$, $sigma_y^*$, $sigma_x^*$ and $sigma_y^*$ equal to zero for TE wave but these are non-zero inside the PML.

This implementation of the PML adds an extra step to the FDTD algorithm, as illustrated in figure 4.4. PML works well in homogeneous media. Problems are caused when there is both dispersive and non-dispersive material at the PML wall. A. P. Zhao [30] introduced a PML algorithm that is material independent and he called it material independent PML. Problem occurs when PML is applied to E and H field because the constant involving this quantity are affected by the material in the simulation space. Therefore in MIPML electric flux density (D) and magnetic flux density(B) are considered for the PML wall for its material independent property. For this reason
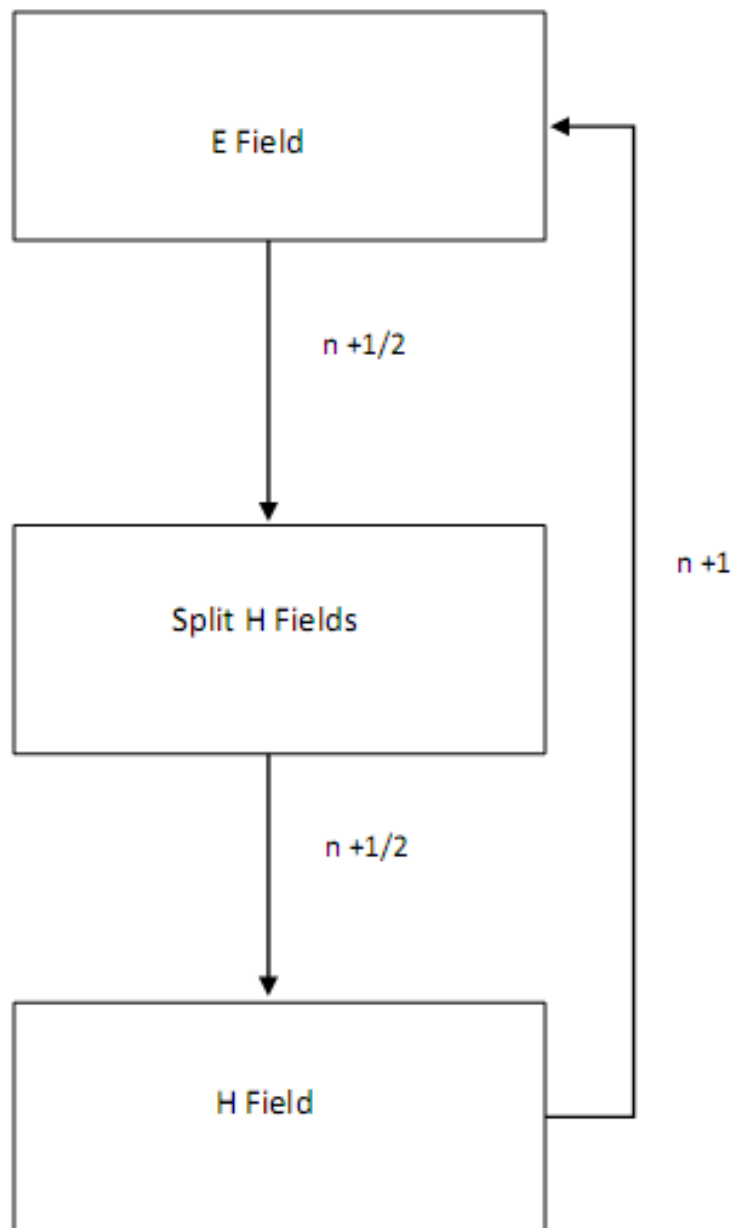
Figure 4.4: FDTD Algorithm Taking Care of PML

new electric and magnetic conductivity are introduced in Maxwells equation.

$$\frac{\partial D_x}{\partial t} + \sigma D_x = \frac{\partial H_z}{\partial y} \tag{4.45}$$

$$\frac{\partial D_y}{\partial t} + \sigma D_y = -\frac{\partial H_z}{\partial x} \tag{4.46}$$

$$\frac{\partial B_z}{\partial t} + \sigma^* B_z = \frac{\partial E_x}{\partial y} - \frac{\partial E_y}{\partial x} \tag{4.47}$$

The condition for impedance matching reduces to $sigma = sigma^*$.
This relation satisfies that electrical conductivity is equal to magnetic conductivity. Moreover the splitting of the fields should also be performed on the D-B layer. Figure 4.5 will describe this phenomena.
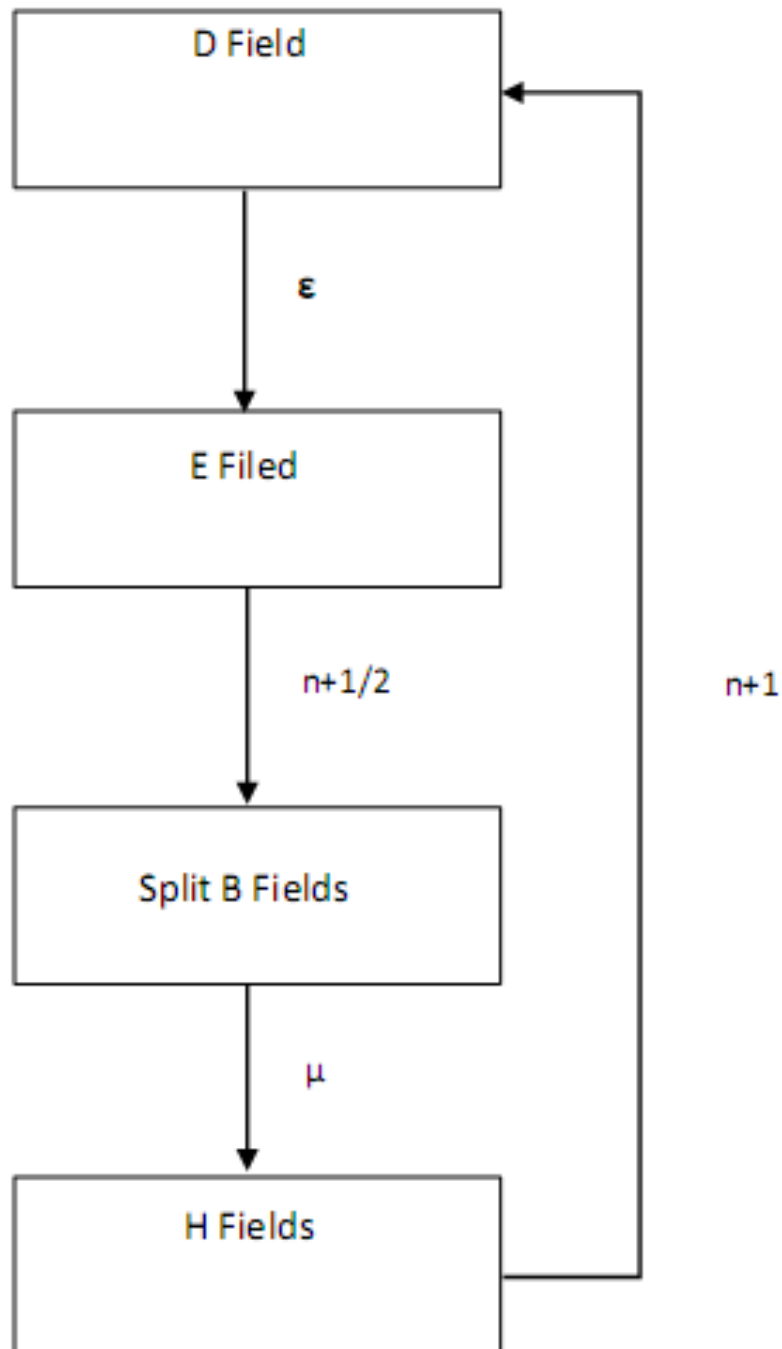
Figure 4.5: MIPML FDTD Algorithm: PML is applied on the B-D level instead of E-H level. In this way, constants in the simulation space are responsible for material properties, and constants in the PML walls are responsible for PML action.

Chapter 5

Bragg Grating

One of the major disadvantages of SPP is that during propagation when it comes to the metal the signal decays very rapidly. From the beginning of the research based on SPP propagation scientists are trying to hold power of the signal when it propagates through the waveguide. Among all the techniques Braggs grating is the most efficient one. The first in-fiber Bragg grating was demonstrated by Ken Hill in 1978. Bragg grating is a device with a periodic variation of the refractive index, so that a large reflectivity may be reached in some wavelength range (bandwidth) around a certain wavelength which fulfills the Bragg condition. The Bragg condition is

$$2d \sin \theta = n\lambda \tag{5.1}$$

It is a type of reflector constructed in a short segment which can reflect the propagated signal to couple it in phase with the forward propagating signal to enhance the signal power i.e. to regain the missing momentum of the SPP. This is achieved by creating a periodic variation in the refractive index by changing the medium of propagation. Bragg grating is often called as Bragg reflector. In this paper Bragg reflector has been analyzed using Metal-Insulator-Metal (MIM) structure at sub wavelength range to increase the propagation distance of the signal [16][17]. Periodic grating scatters light in the homogeneous media which leads to the concept of Photonic Band Gap (PBG). Photonic Band gap is a term applicable to the dielectric media which possesses alternate region of low and high refractive index such that transmission of photons or light energy of certain frequencies is forbidden. Thus it is a photon forbidden region in the case of electron band gap of the semiconductor. Here, we have used AlgaAs as the background material. Because of the ultrafast nonlinear property, we have used GLS [14] and Cu_2O for forming gratings. It can be coupled with silver to propagate SPP more efficiently.

5.1 Metal insulator relation

The values of the dielectric constant can be taken from the fitted curve which has already been published in different journals or papers. The other way is to calculate it using mathematical formula. It can be calculated from the refractive index of different dielectric materials. The dielectric constant for any material can be expressed as,

$$\varepsilon_1 = n^2 - k^2 \tag{5.2}$$

Table 5.1: Parameters for Different Dielectrics

Insulators	ε_0	ε_∞	ω_0	Delta
AlGaAs	2.88^2	1.24^2	0.65×10^{16}	6×10^{13}
Cu_2O	2.49^2	1.41^2	0.53×10^{16}	6.1×10^{10}
GLS	2.257^2	2.7	0.7×10^{16}	8×10^{11}

$$\varepsilon_2 = 2nk \tag{5.3}$$

Where ϵ_1 and ϵ_2 are the real and imaginary parts of the dielectric constant. n and k are the real and imaginary parts of the refractive index. The dispersion relation of the dielectric material used in this paper is incorporated in the FDTD simulator using Auxiliary Differential Equation (ADE) technique. The frequency dependent refractive index of silver has been taken from [25]. Using the dispersion relation mentioned in [24], the complex effective refractive index, N_{eff} can be expressed as,

$$N_{eff} = \frac{\beta}{\beta_0} = \sqrt{\frac{\varepsilon_d \varepsilon_m}{\varepsilon_d + \varepsilon_m}} \tag{5.4}$$

Where, ϵ_d and ϵ_m are the dielectric constants of the dielectric and metal respectively. β is the complex propagation constant of the wave guide and β_0 is the complex propagation constant of the free space. The dielectric parameters to fit the single pole Lorentz model for different dielectrics are given in table 5.1.

5.2 Grating structure

We considered a metal thin film sandwiched between two dielectric layers with different dielectric grating. Figure 5.1 shows the resulting geometry of the proposed structure, which is considered to be infinite along the y -direction.

The guided SPP propagates along the metal-dielectric interface. A transverse magnetic (TM) polarized mode modulated by a Gaussian pulse is pumped at $x = 0$ and time $t = 0$. The thickness (t_p) of the metal thin film has been varied to observe the propagation efficiencies for different dielectric materials. The reason of using this grating structure in this paper is to produce an efficient SPP mode with low loss. The grating is characterized by the insulation section length $(\Delta_{1,2})$ which can be obtained by the Bragg condition [22] ,

$$\Delta_{1,2} = \frac{\lambda}{4\mathrm{Re}(N_{eff1,2})} \tag{5.5}$$

Where $N_{eff1,2}$ is the Effective Refractive Index (ERI) and λ is the central wavelength. The role of the grating is to provide the missing momentum of the SPP. Complex mode matching method [21] is used to investigate the grating structure where the boundary is determined by a perfectly matched layer (PML). An efficient SPP propagation is expected provided that the SPP wave satisfies the complex mode matching conditions.
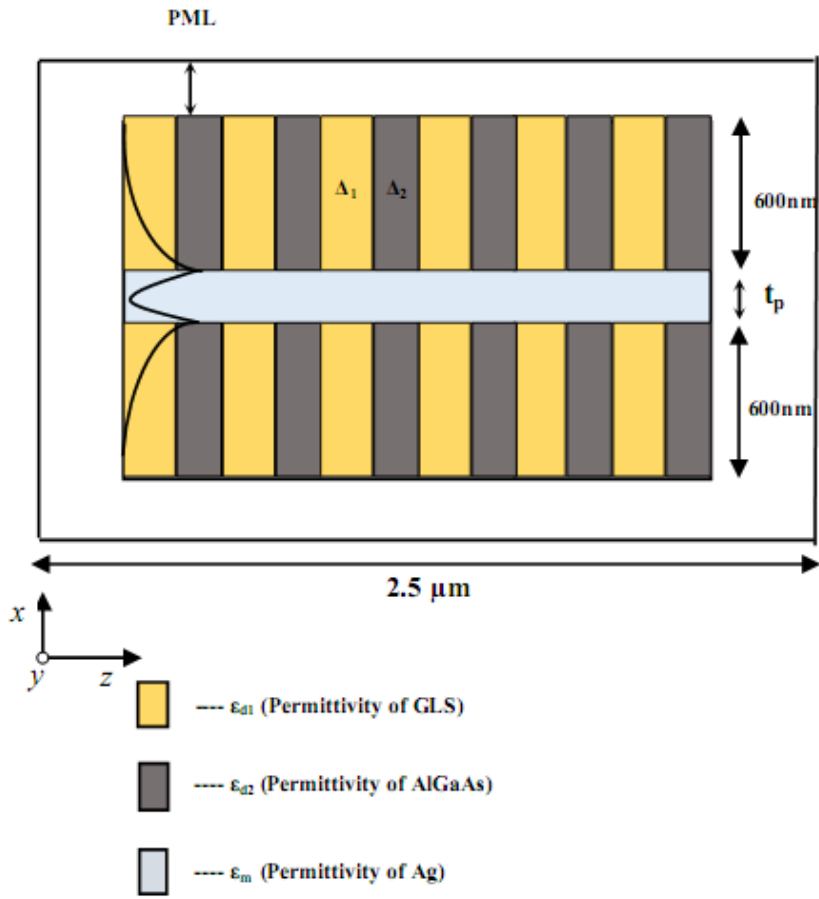
Figure 5.1: Grating structure

Chapter 6

Numerical Results

During the time of our thesis we have performed several simulations to enhance our knowledge on the coding scheme and as well as to familiarize with the fabrication based research work. In our thesis for computation purpose we choose FDTD for its various advantages. With the help of those simulations we have got the idea of different signals behavior when they propagate through the dielectric medium. At the first part we have simulated 1-dimensional FDTD and then two dimensional FDTD. In both the cases air was used as the dielectric medium and the signal has been generated at the middle of the computational window. In the simulation Gaussian pulse has been used because it does not produce any side lobe in the frequency domain as compared with the rectangular pulse. For 1-dimensional case at first we have simulated without considering the polarization. Simulation results are presented by figure 6.1.

Now we have to consider the loss properties inside the material. To describe loss property let us introduce the term polarization. Polarization is described as the orientation of the oscillation of waves inside the material when external electric field is applied. So when the polarization is considered then we can observe how the signal decays when it is propagating through the medium. Simulation results after considering polarization is presented by figure 6.2a.
In order to test our simulation for one dimensional FDTD we used the data given by Allen Taflove [1]. The simulated results using our developed simulator, give a very good agreement with the published results. The simulated results from Tafloves book [1] and our simulator is given by figure 6.2.
 For 2-dimensional FDTD the simulation results are shown by figure 6.1.
  We pumped a Gaussian pulse at the middle of the dielectric. When the signal propagates, it reflects back due to the absence of Perfectly Matched Layer (PML). Figure 6.2c shows the reflected signal from the boundary of the computational window. In the above figures different colors are demonstrating the strength of the signal at different places. Red color is representing the maximum power and the blue color is representing the minimum power of the signal.
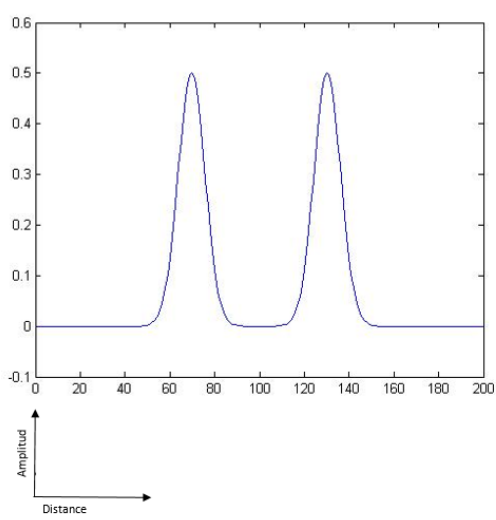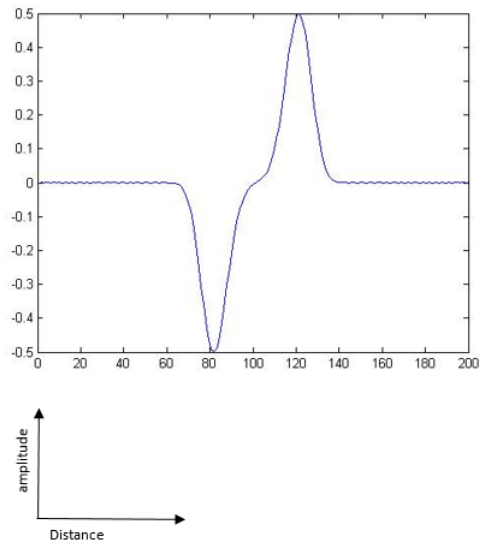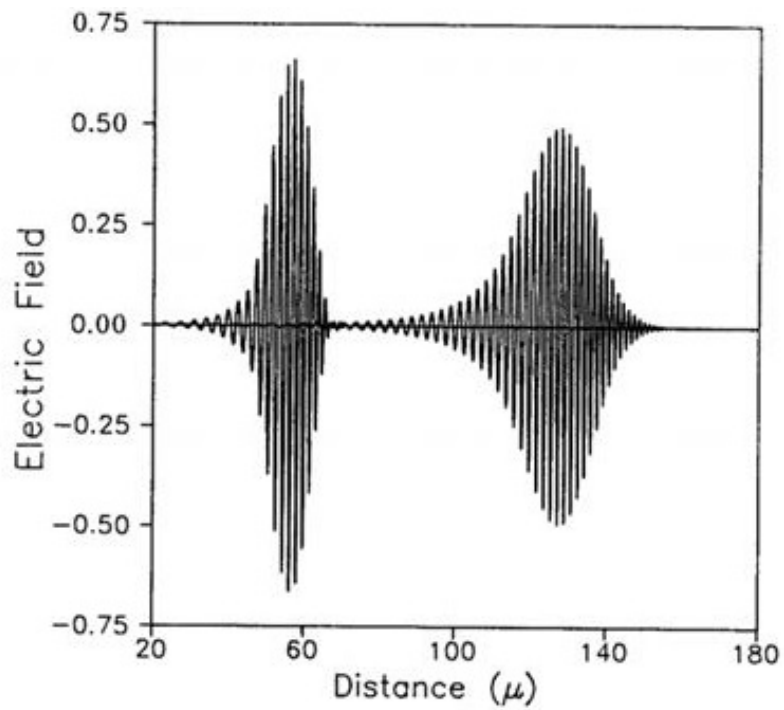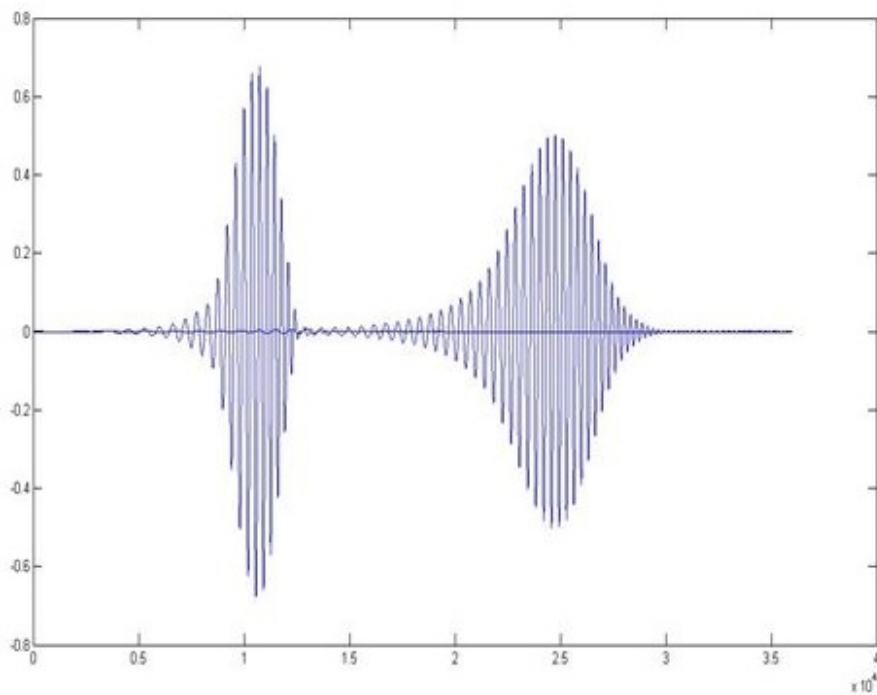
(a) Figure a
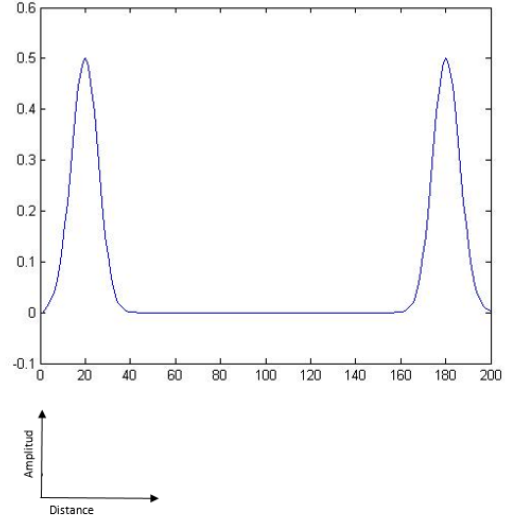
(b) Figure b
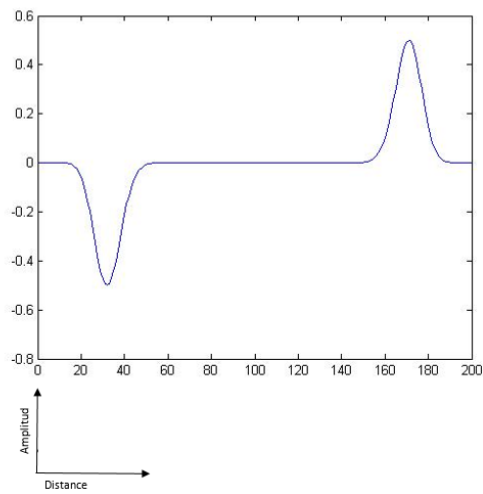
(c) Figure c

(d) Figure d

Figure 6.1: Signal propagation in 1 dimensional FDTD: (a) After 0.83 ns (b) After 1.6 ns (c) After 2.4 ns (d) After 3.3 ns
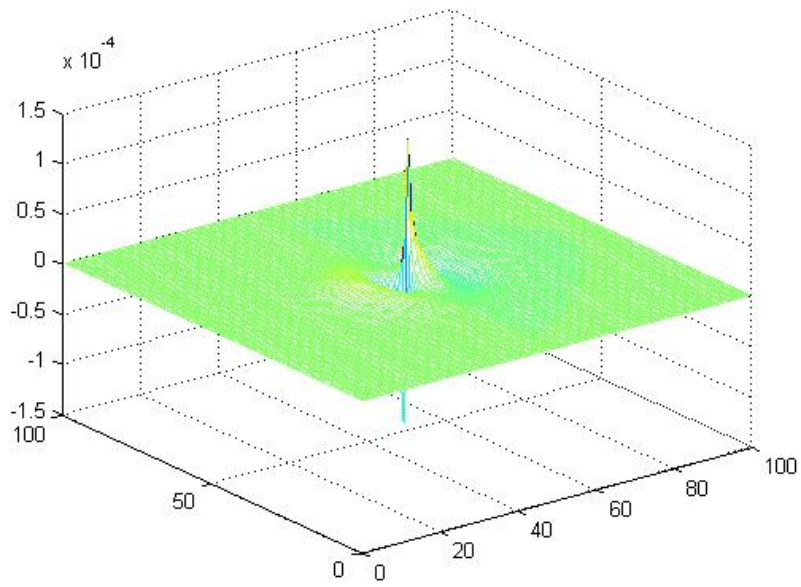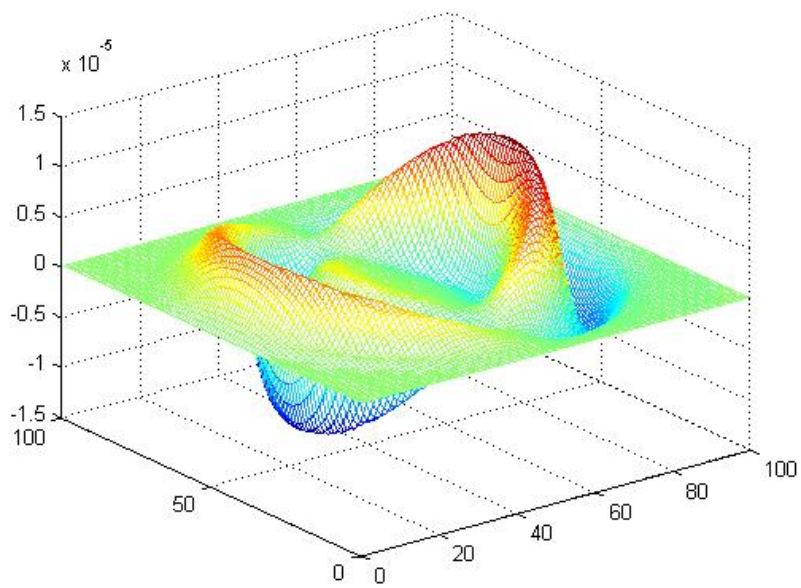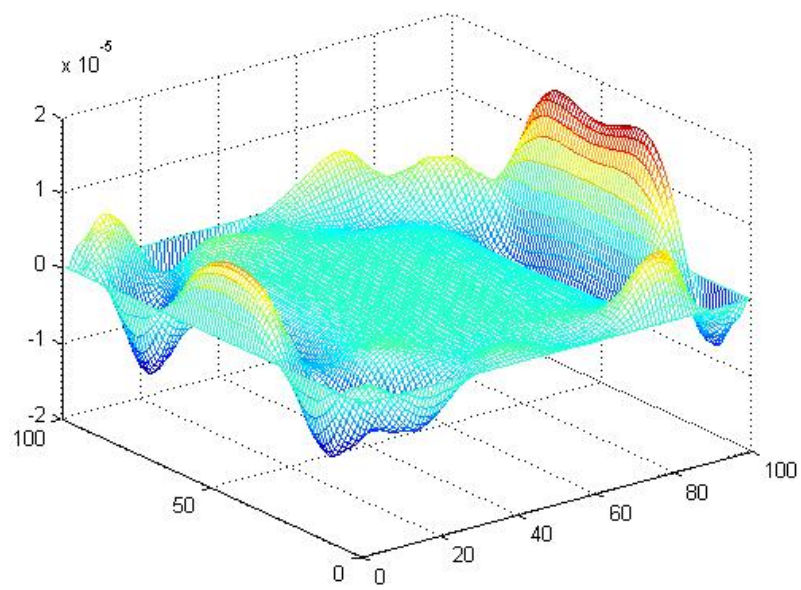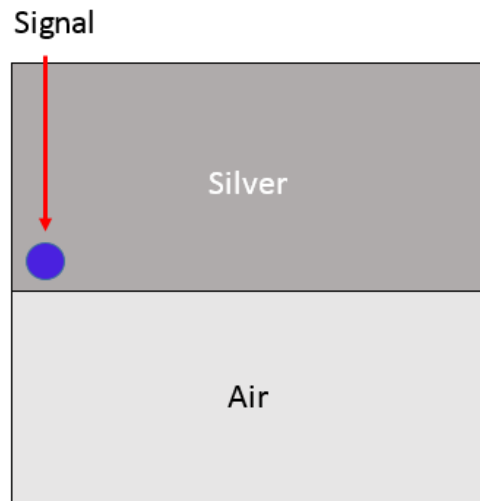
(a) Figure a

(b) Figure b

Figure 6.2: ADE-FDTD study of temporal soliton formation in a nonphysical nonlinear dispersive medium: (a) Calculated optical carrier pulse after propagating 126 μm (b) Similar figure using our own developed simulator.

(a) Figure a

(b) Figure b

(c) Figure c

Figure 6.1: Signal propagation in 1 dimensional FDTD.: (a) After 0.41 ns (b) After 0.83 ns (c) After 1.24 ns

Figure 6.2: A Metal Dielectric Interface.

6.1 SPP Simulation

In the second phase SPP simulations are performed by forming the interface between dielectric and metal. PML has been used to terminate the propagating signal within the computational window. For better understanding of SPP the concept of waveguide is very important. It plays a very vital role to transmit the signal at sub wavelength range. At first a very simple waveguide has been designed by forming an interface between metal and dielectric. Silver has been used for the metal and Lorentz-Drude 6 pole model has been used to design it. All the parameters for the dielectric have been taken from the published research papers. The simulation results are shown by figures 6.2, 6.3, and 6.2.
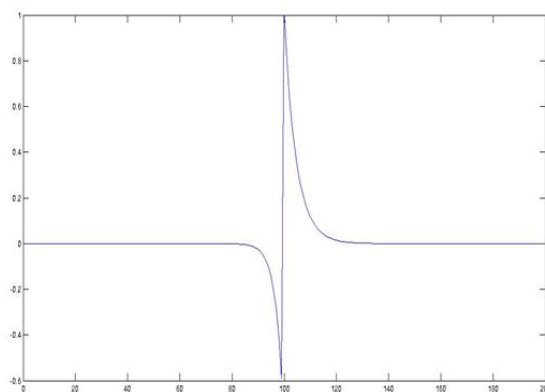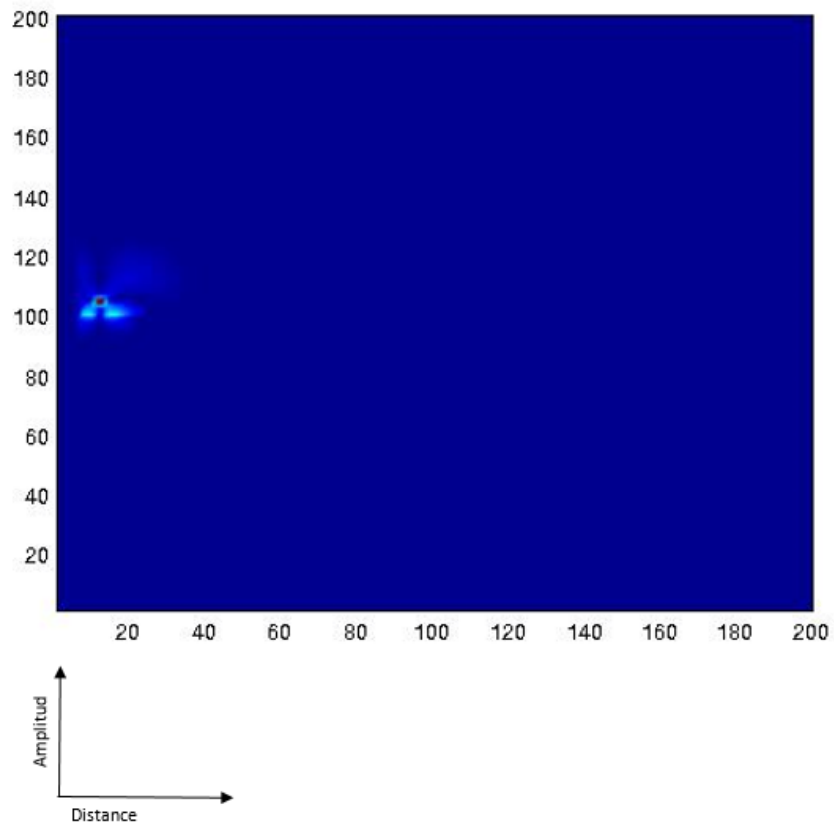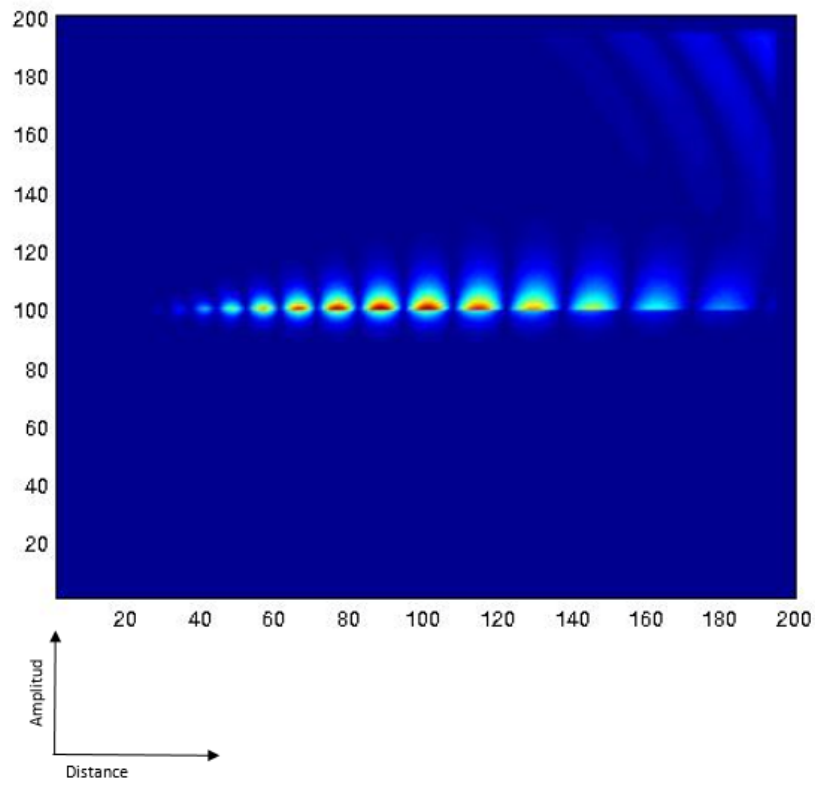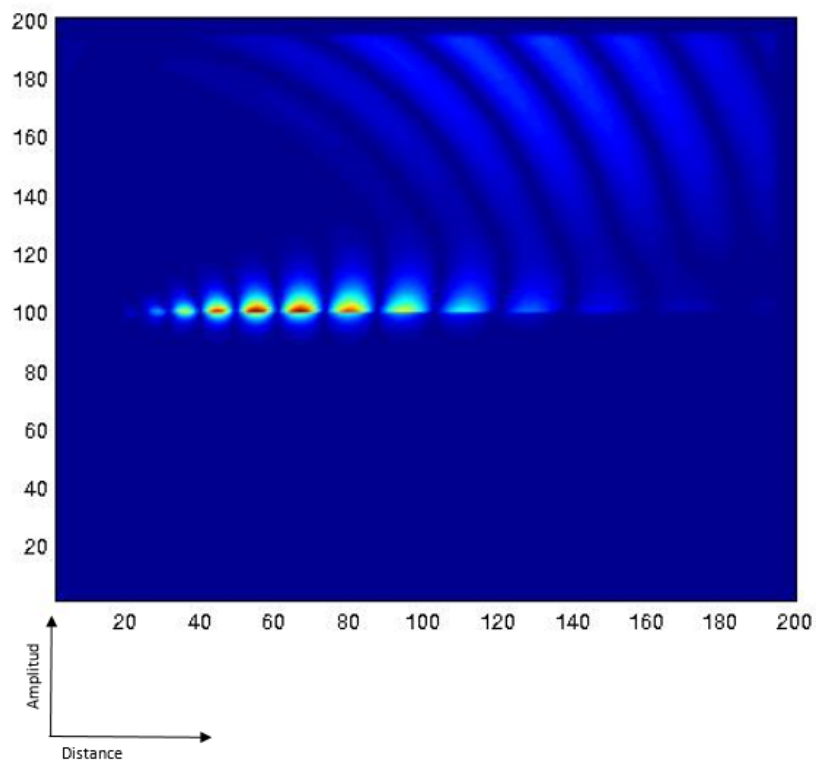

Figure 6.3: Profile of the Metal Dielectric interface.

(a) Figure a

(b) Figure b

(c) Figure c

Figure 6.2: Signal propagation in Metal Dielectric interface: (a) After 35.525 fs (b) After 177.625 fs (c) After 106.56 fs
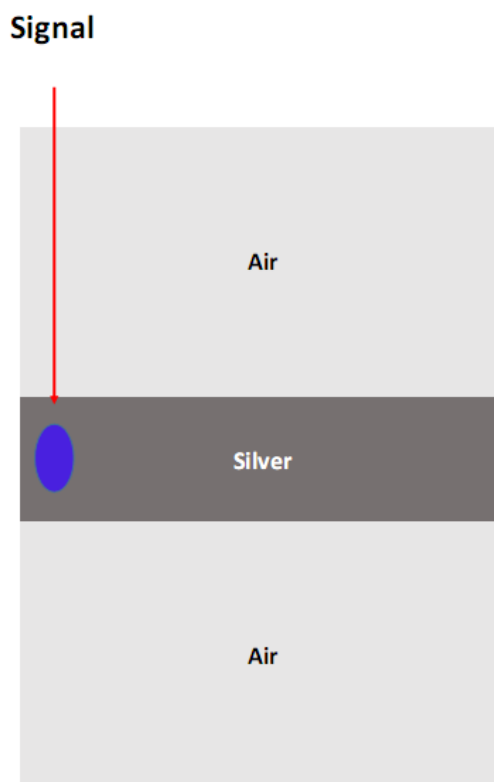
Signal

Figure 6.3: A Dielectric Metal Dielectric Interface.

Here, figure 6.3 represents the profile of the signal. The profile of the signal represents the signal decaying in a material.
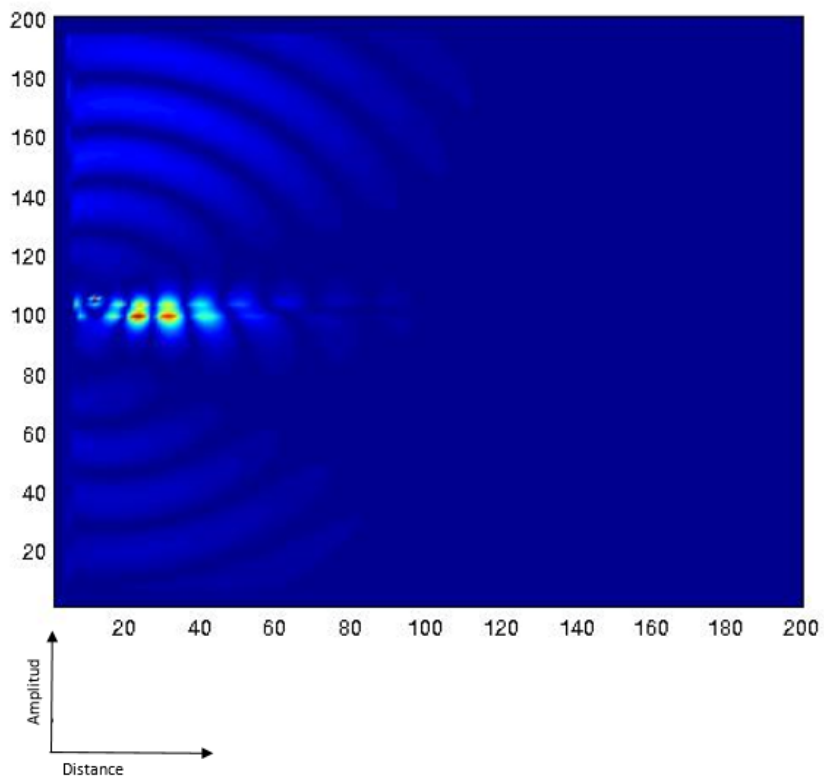
Metal dielectric Metal (MDM) and Dielectric Metal Dielectric (DMD) have also been simulated to see the propagation through the double interface. For both the structure AlGaAs has been used as the dielectric material and Silver has been used as the metal. The simulation results for the DMD are shown by figures 6.3 and 6.2.

The simulation result for the MDM are shown by figures 6.3 and 6.2

In our consideration the signal propagates along the z direction. During transmission, part of the signal is transmitted and others are reflected. There will be absorption and radiation loss of the signal during transmission through grating structure.

In the final phase of our work we have focused on Braggs grating because of its ability to enhance power. We have experimented on GLS and $AlGaAs$ to show the enhancement of the power.

We have calculated power transmission for different metallic strip thicknesses as a function of transmission distance. Figure 6.3 represents the transmitted power at different distances: $d_1 = 500nm$, $d_2 = 1000nm$, $d_3 = 1500nm$ and $d_4 = 2000nm$ for different metallic strip thicknesses t_p. It is seen from the graph that the power decreases as the distance increases and in every case it is maximum for $50nm$ metallic strip. Observation reveals that the field penetration decreases with the increase of the metal width within the dielectric grating structure as shown by figure 5.1. For $50nm$ metallic strip resonance is created by the signal which causes the power
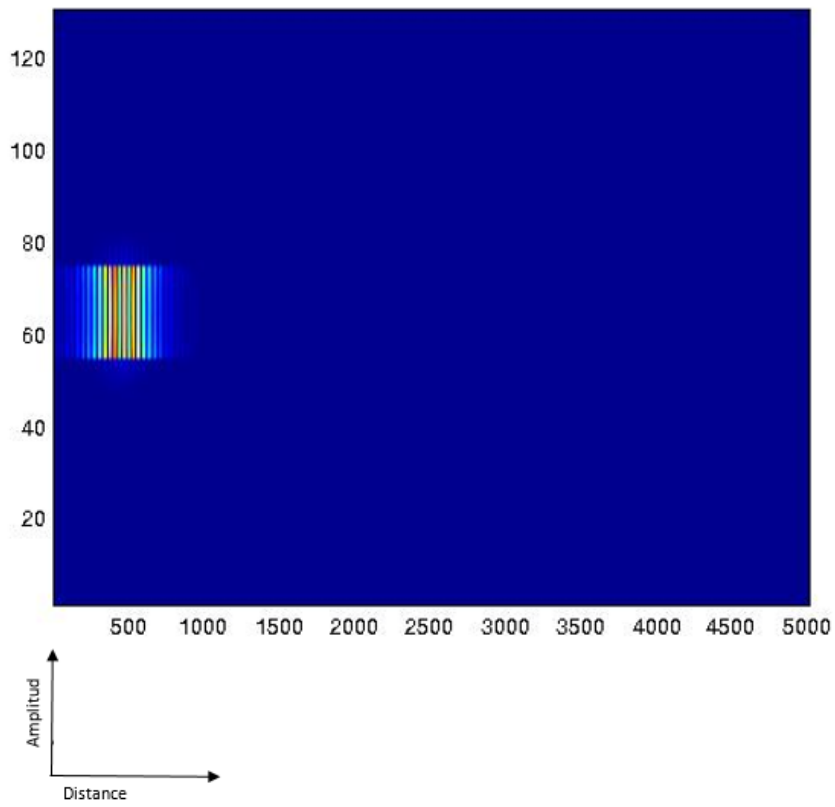
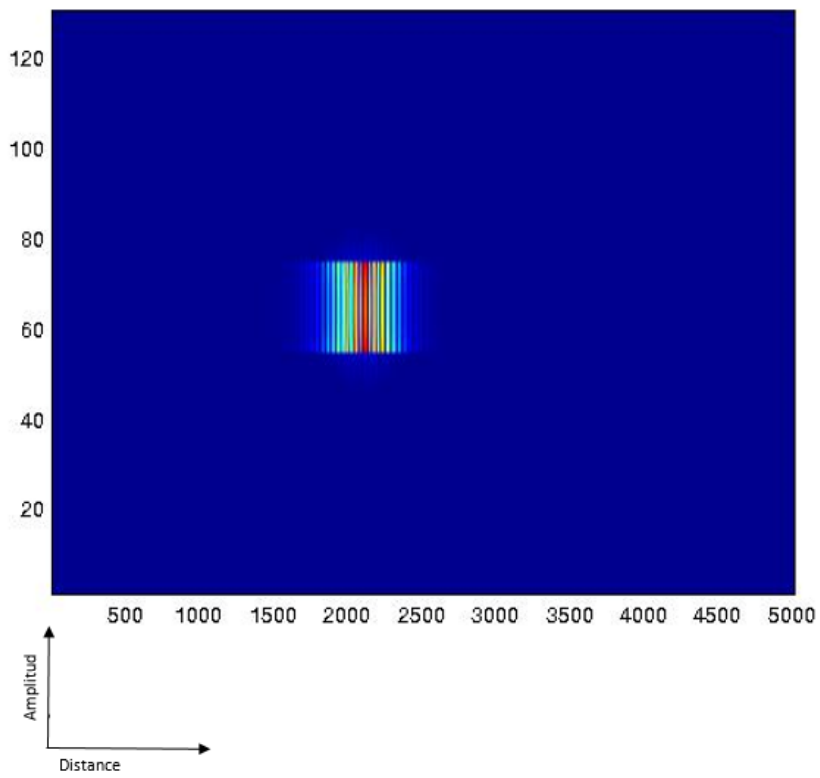(a) Figure a
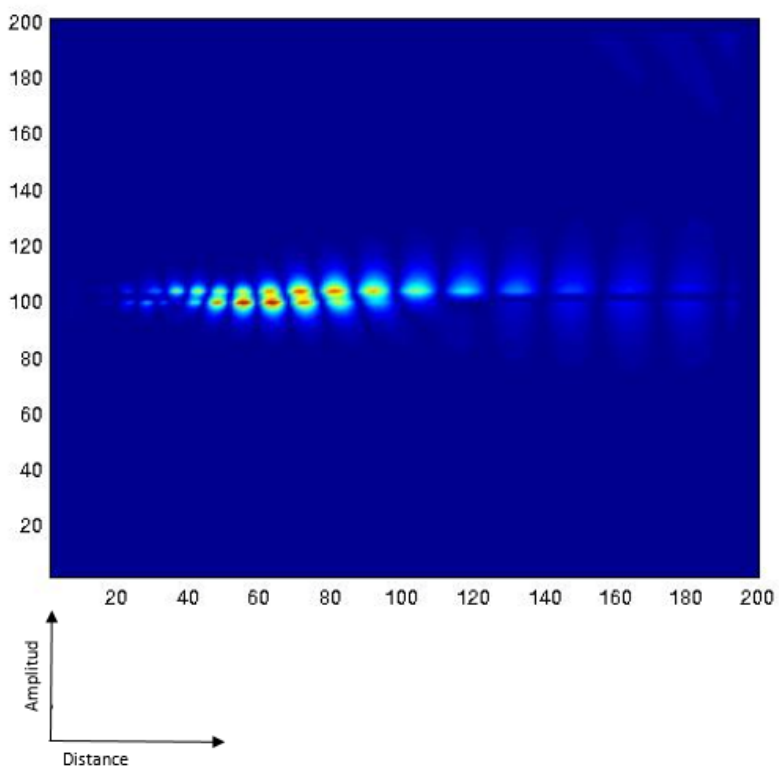
(b) Figure b
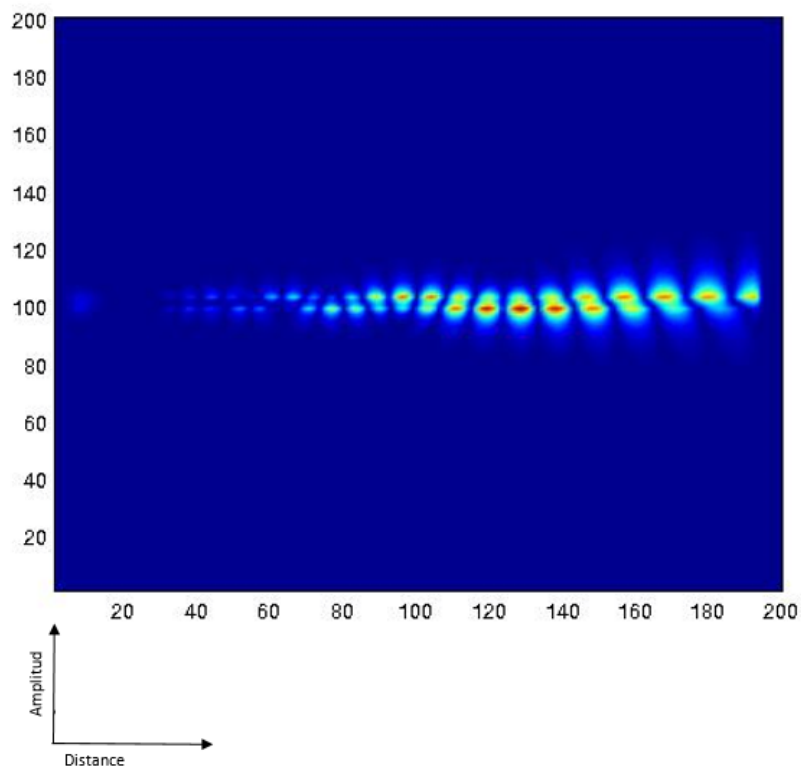
(c) Figure c

Figure 6.2: Signal propagation in Dielectric Metal Dielectric interface: (a) After 180.26 fs (b) After 360.53 fs (c) After 288.42 fs
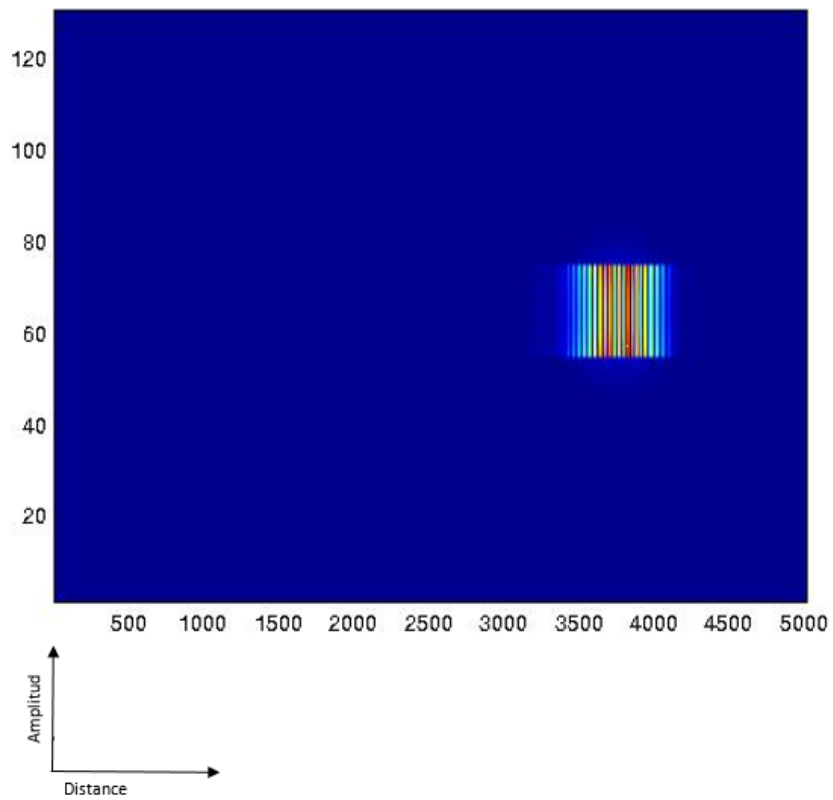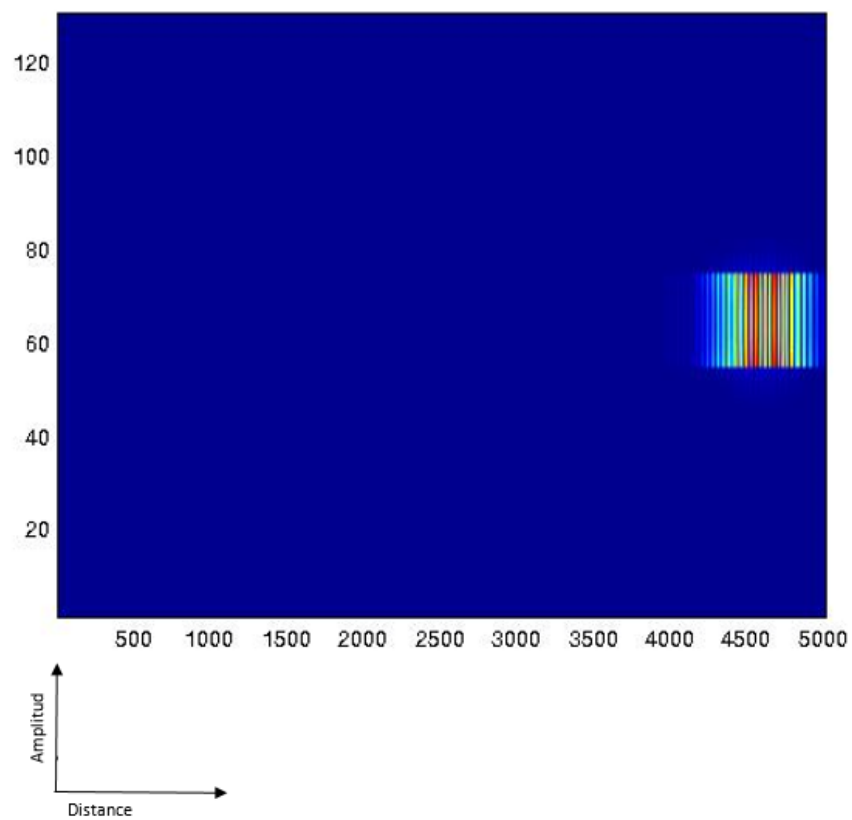

Figure 6.3: Metal Dielectric Metal Interface.

(a) Figure a

(b) Figure b

(c) Figure c

42

(d) Figure d

Figure 6.2: Signal propagation in Metal Dielectric Metal Interface: (a) After 87 fs (b)After 175 fs (c) After 263 fs (d) After 307 fs
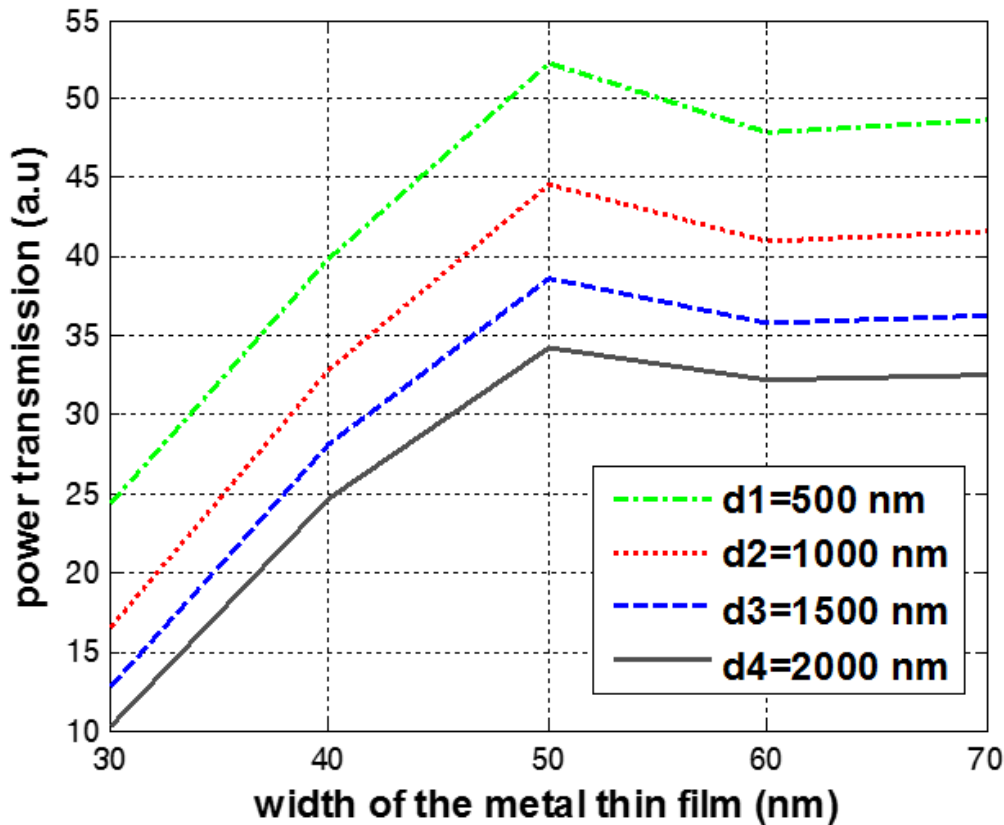
Figure 6.3: Comparison of power transmission for different material width.

to enhance during propagation. Grating helps the metal strip to select an appropriate mode for efficient propagation of the signal. The results have been taken for a fixed wavelength $1550nm$.

Next, the comparison of the power transmission and loss between the two dielectrics, Gallium Lanthanum Sulphide (GLS) and Cuprous Oxide (Cu_2O) has been investigated. We have taken (Cu_2O) to compare with GLS in order to find dielectric which gives low loss property. Here the transmission and loss properties have been calculated numerically with graphical representation. The analysis is performed for a constant metallic strip thickness ($50nm$) because of its maximum transmission rate in figure 6.3. In figure 6.4 it is observed that Cuprous Oxide can transmit more power during transmission of the signal. In 6.5 it is shown that with the increase of the wavelength the loss for GLS gradually increases compared to (Cu_2O).The results have been taken for different wavelength starting from $1400nm$ to $1600nm$.

Because of the low loss property (Cu_2O) can hold more power and this result is convenient for all other wavelengths.
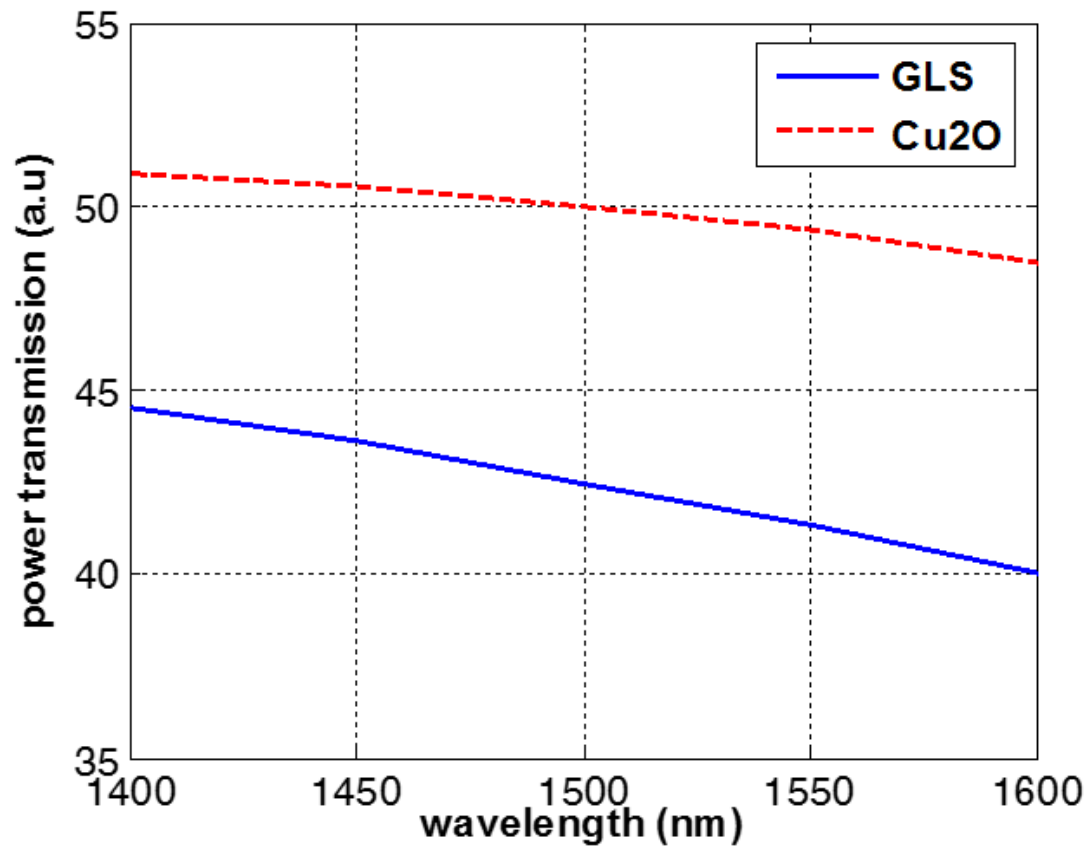
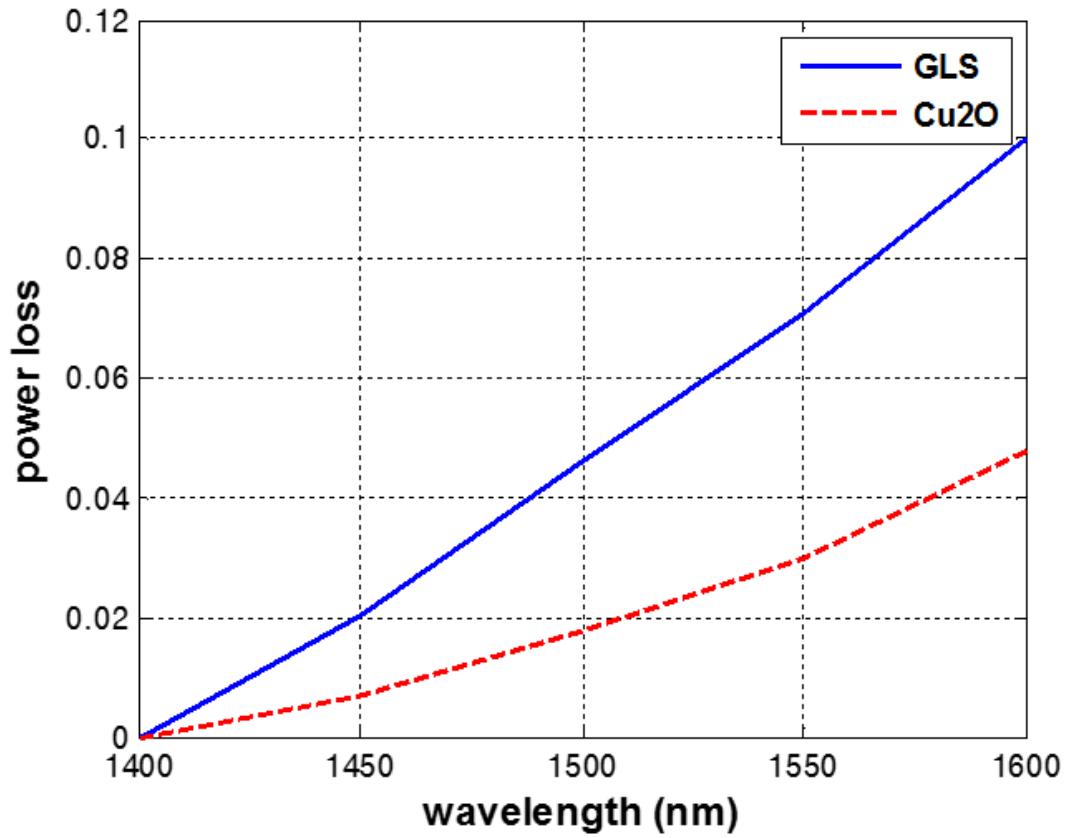Figure 6.4: Comparison of power transmission for different dielectrics (GLS and Cu_2O).

Figure 6.5: Comparison of power loss for different dielectrics (GLS and Cu_2O).

Chapter 7

Conclusion

7.1 Conclusion

Our research is based on the investigation of efficient SPP propagation. Before starting with the SPP we have studied theoretical analysis of the different computational technique. Summary of the thesis work is presented below:

1. An investigation has been performed on the efficient algorithm to design the material. Different models have been analyzed out of which Lorentz model has been taken to design the dielectric and Lorentz Drude 6 pole models has been used to design the metal. To avoid the complex mathematics ADE based algorithm has been used to design the multiple dispersion relation.

2. In our simulations we have created SPP at the metal dielectric interface and observe the signal behavior for single and double interfaces. FDTD based simulations have also been performed to observe the propagation of signal within the dielectric material.

3. Grating structure has been analyzed with a view to hold signal power for longer distance. We have also investigated the structure numerically and graphically to get a clear idea how grating increase power within the computational window.

7.2 Future Work

1. Due to the high loss property of the metal at high frequency the propagating signal cannot sustain so long. Up to now maximum possible distance used for scientific research is 6-7 μm. Grating is one of the good solution to do this. So our future plan is to increase the propagation distance by investigating the nature of the grating. Grating structure will be improved if new dielectric with low loss is used to design it.

2. Material modeling is a very important aspect in Plasmonics. If new material can be developed then it will be possible to sustain the signal for long duration.

46

3. As photon has the advantages over electron in terms of high speed and low heat generation capacity this research work will be highly efficient for miniaturization of photonic devices. Increasing propagation distance can also be a great contribution to the field of communication especially in optically controlled devices.

Bibliography

[1] Allen Taflove and Susan C. Hagness, *COMPUTATIONAL ELECTRODYNAMICS: THE FINITE-DIFFERENCE TIME-DOMAIN METHOD*, 3rd ed. 2000 ARTECH HOUSE INC, 2005.

[2] M. A. Alsunaidi and A. A. Al Jabr, "A general ADE-FDTD algorithm for the simulation of dispersive structures," *Photonics Technology Letters, IEEE*, vol. 21, no. 12, pp. 817–819, 2009.

[3] C. A. Balanis, *Advanced engineering electromagnetics*. Wiley New York, 1989, vol. 205.

[4] W. L. Barnes, A. Dereux, and T. W. Ebbesen, "Surface plasmon subwavelength optics," *Nature*, vol. 424, no. 6950, pp. 824–830, 2003.

[5] J.-P. Berenger, "A perfectly matched layer for the absorption of electromagnetic waves," *Journal of computational physics*, vol. 114, no. 2, pp. 185–200, 1994.

[6] J.-L. Chabert and É. Barbin, *A history of algorithms*. Springer, 1999.

[7] L. Chen, J. Shakya, and M. Lipson, "Subwavelength confinement in an integrated metal slot waveguide on silicon," *Optics letters*, vol. 31, no. 14, pp. 2133–2135, 2006.

[8] P. Drude, "Zur elektronentheorie der metalle," *Annalen der Physik*, vol. 306, no. 3, pp. 566–613, 1900.

[9] ——, "Zur elektronentheorie der metalle; II. Teil. galvanomagnetische und thermomagnetische effecte," *Annalen der Physik*, vol. 308, no. 11, pp. 369–402, 1900.

[10] C. H. Edwards Jr, *The historical development of the calculus*. Springer, 1979.

[11] G. Gay, O. Alloschery, B. V. De Lesegno, C. Odwyer, J. Weiner, and H. Lezec, "The optical response of nanostructured surfaces and the composite diffracted evanescent wave model," *Nature Physics*, vol. 2, no. 4, pp. 262–267, 2006.

[12] S. Hamdi, W. E. Schiesser, and G. W. Griffiths, "Method of lines," *Scholarpedia*, vol. 2, no. 7, p. 2859, 2007.

[13] Y. Hao and R. Mittra, *FDTD modeling of metamaterials*. Artech house, 2009.

[14] R. HasanSagor, "Plasmon Enhanced Symmetric Mode Generation in Metal-Insulator-Metal Structure with Kerr Nonlinear Effect," *International Journal of Computer Applications*, vol. 50, no. 18, pp. 24–28, 2012.

[15] M. Hochberg, T. Baehr Jones, C. Walker, and A. Scherer, "Integrated plasmon and dielectric waveguides," *Optics Express*, vol. 12, no. 22, pp. 5481–5486, 2004.

[16] A. Hosseini and Y. Massoud, "A low-loss metal-insulator-metal plasmonic bragg reflector," *Optics express*, vol. 14, no. 23, pp. 11 318–11 323, 2006.

[17] J. T. Kim, J. J. Ju, S. Park, M.-s. Kim, S. K. Park, and S.-Y. Shin, "Hybrid plasmonic waveguide for low-loss lightwave guiding," *Optics express*, vol. 18, no. 3, pp. 2808–2813, 2010.

[18] K. Lee and Q.-H. Park, "Coupling of surface plasmon polaritons and light in metallic nanoslits," *Physical review letters*, vol. 95, no. 10, p. 103902, 2005.

[19] S. A. Maier, "Plasmonics: The promise of highly integrated optical devices," *Selected Topics in Quantum Electronics, IEEE Journal of*, vol. 12, no. 6, pp. 1671–1677, 2006.

[20] N. S. Matthew and O. Sadiku, "Numerical techniques in electromagnetics," *2ND, EDITION, CRC PRESS, ISBN 0-8493-1395-3*, 2001.

[21] J.-W. Mu and W.-P. Huang, "Simulation of surface plasmon polariton (SPP) Bragg gratings by complex mode matching method," *Integrated Photonics and Nanophotonics Research and Applications*, 2007.

[22] ——, "A low-loss surface plasmonic Bragg grating," *Journal of Lightwave Technology*, vol. 27, no. 4, pp. 436–439, 2009.

[23] T. Onuki, Y. Watanabe, K. Nishio, T. Tsuchiya, T. Tani, and T. Tokizaki, "Propagation of surface plasmon polariton in nanometre-sized metal-clad optical waveguides," *Journal of microscopy*, vol. 210, no. 3, pp. 284–287, 2003.

[24] H. Raether, *Surface plasmons on smooth surfaces*. Springer, 1988.

[25] A. D. Rakic, A. B. Djurišic, J. M. Elazar, and M. L. Majewski, "Optical properties of metallic films for vertical-cavity optoelectronic devices," *Applied optics*, vol. 37, no. 22, pp. 5271–5283, 1998.

[26] J. N. Reddy, *An introduction to the finite element method*. McGraw-Hill New York, 2006, vol. 2.

[27] W. E. Schiesser and G. W. Griffiths, *A compendium of partial differential equation models: method of lines analysis with Matlab*. Cambridge University Press, 2009.

[28] W. E. Schiesser and W. E. Schiesser, *The numerical method of lines: integration of partial differential equations*. Academic Press San Diego, 1991, vol. 212.

[29] D. M. Sullivan, "Frequency-Dependent FDTD Method Using Z-Transform," *Antennas & Propagation, IEEE Transactions on*, vol. 40, no. 10, pp. 1223–1230, 1992.

[30] A. Zhao, J. Juntunen, and A. Raisanen, "Material independent PML absorbers for arbitrary anisotropic dielectric media," *Electronics Letters*, vol. 33, no. 18, pp. 1535–1536, 1997.